KADIR HAS UNIVERSITY
SCHOOL OF GRADUATE STUDIES
DEPARTMENT OF ENGINEERING AND NATURAL SCIENCES

THE OPTICAL AND ELECTRICAL CHARACTERISTICS OF ZnO/MoS_2 TRANSPARENT OXIDE COMPOSITE FILMS

SHAHAD TAREQ
Assoc. Prof. Dr. GÖKHAN KİRKİL
Assoc. Prof. Dr. BENGÜ ÖZUĞUR UYSAL

MASTER'S DEGREE THESIS

ISTANBUL, FEBERURY, 2021

THE OPTICAL AND ELECTRICAL CHARACTERISTICS OF ZnO/MoS_2 TRANSPARENT OXIDE COMPOSITE FILMS

SHAHAD TAREQ
Assoc. Prof. Dr. GÖKHAN KİRKİL
Assoc. Prof. Dr. BENGÜ ÖZUĞUR UYSAL

MASTER'S DEGREE THESIS

SUBMITTED TO THE SCHOOL OF GRADUATE STUDIES
WITH THE AIM TO MEET THE PARTIAL REQUIREMENTS REQUIRED TO
RECEIVE A MASTER'S IN THE DEPARTMENT OF ENGINEERING AND
NATURAL SCIENCES

ISTANBUL, FEBERURY, 2021

NOTICE ON RESEARCH ETHICS AND
PUBLISHING METHODS

I, SHAHAD TAREQ;

- hereby acknowledge, agree and undertake that this Master's Degree Thesis that I have prepared is entirely my own work and I have declared the citations from other studies in the bibliography in accordance with the rules;
- that this Master's Degree Thesis does not contain any material from any research submitted or accepted to obtain a degree or diploma at another educational institution;
- and that I commit and undertake to follow the "Kadir Has University Academic Codes of Conduct" prepared in accordance with the "Higher Education Council Codes of Conduct".

In addition, I acknowledge that any claim of irregularity that may arise in relation to this work will result in a disciplinary action in accordance with the university legislation.

SHAHAD TAREQ

_____

DATE AND SIGNATURE

ACCEPTANCE AND APPROVAL

This study, titled **THE OPTICAL AND ELECTRICAL CHARACTERISTICS OF ZnO/MoS_2 TRANSPARENT OXIDE COMPOSITE FILMS**, prepared by the **SHAHAD TAREQ**, was deemed successful with the **UNANIMOUS/MAJORITY VOTING** as a result of the thesis defense examination held on the **11 February 2021** and approved as a **MASTER'S DEGREE THESIS** by our jury.

JURY:

SIGNATURE:

Assoc. Prof. Dr. Gökhan Kirkil Kadir Has University _____

Assoc. Prof. Dr. Bengü Özuğur Uysal Kadir Has University _____

Asst. Prof. Dr. Emre Ozan Polat Kadir Has University _____

Prof. Dr. Esra Zayim Istanbul Technical University_____

Asst. Prof. Dr. Hakan Kaygusuz Altınbaş University _____

I confirm that the signatures above belong to the aforementioned faculty members.

_____

(Title, Name and Surname)

Director of the School of Graduate Studies

APPROVAL DATE: Day/Month/Year

TABLE of CONTENTS

THE OPTICAL AND ELECTRICAL CHARACTERISTICS OF ZnO/MoS_2 TRANSPARENT OXIDE COMPOSITE FILMS

ABSTRACT

The use of transparent conductive oxide in optoelectronics creates a revolution where new generation materials with high transmittance and low sheet resistance value, durability and portability are achieved without decreasing efficiency or increasing cost. ZnO / MoS_2 transparent conductive composite films was produced by the sol-gel method, which is considered the most important method due to its simple process and low cost. The crystal structure properties of ZnO / MoS_2 have been characterized by the X-Ray diffraction pattern (XRD). The crystal size of ZnO film doped with different amounts of MoS_2 was determined by XRD spectroscopy. UV-visible absorption spectrometer was used to perform spectroscopic analysis of the film. The area under the absorption curve and the full width of the half maximal absorbance data were calculated. Using this value, MoS_2 amount was determined for the best additive distribution. In addition, in order to determine the best transparent conductive material, the resistance values obtained by using the four-point probe method were compared for different MoS_2 additive amounts. The optical and electrical characterizations of ZnO / MoS_2 transparent conductive oxide film were investigated.

Keywords: thin film, sol-gel, transparent conducting oxide, ZnO/MoS_2 composite.

ZnO/MoS_2 SAYDAM OKSİT KOMPOZİT FİLMLERİN OPTİK VE ELEKTRİKSEL KARAKTERİSTİKLERİ

ÖZET

Optoelektronikte saydam iletken oksit kullanımı, verimliliği düşürmeden veya maliyeti artırmadan esneklik, dayanıklılık ve taşınabilirlik becerisinin elde edildiği bir devrim yaratmaktadır.

ZnO / MoS_2 saydam iletken kompozit filmi basit bir süreç oluşu ve düşük maliyeti nedeniyle en önemli yöntem olarak kabul edilen sol-jel yöntemi ile üretilmiştir. ZnO / MoS_2'nin kristal yapı özellikleri, X-Işını kırınım modeli (XRD) ile karakterize edilmiştir. XRD spektroskopisi ile, farklı miktarlarda MoS_2 katkılı ZnO filminin kristal boyutu tayin edilmiştir. UV- görünür bölge absorpsiyon spektrometresi, filmin spektroskopik analizini gerçekleştirmek için kullanılmıştır. Absorpsiyon eğrisinin altındaki alan ve yarı maksimum absorbans verilerinin tam genişliği hesaplanmıştır. Bu değerle kullanılarak en iyi katkı maddesi dağılımı için MoS_2 miktarı tespit edilmiştir. Ayrıca, en iyi saydam iletken malzemeyi belirlemek üzere, dört nokta prob yöntemi kullanılarak elde edilen direnç değerleri farklı MoS_2 katkı miktarları için kıyaslanmıştır. Bu çalışmada, bir ZnO / MoS_2 saydam iletken oksit filmin optik ve elektrik karakterizasyonlarını incelenmiştir.

Anahtar Kelimeler: ince film, sol-jel, geçirgenlik, şeffaf iletken oksit, ZnO./MoS_2 kompoziti

ACKNOWLEDGEMENT

My deepest gratitude to my supervisors, **(Assoc. Prof. Dr. GÖKHAN KİRKİL)** and **(Assoc. Prof. Dr. BENGÜ ÖZUĞUR UYSAL)** for the continuous support of my Master's thesis, for their patience, motivation, enthusiasm, and immense knowledge. Their guidance helped me in all the time of research and writing of this thesis.

I would like to express my sincere thanks to **(Dr. Taner Arsan)** and the entire faculty members of the Electrical-Electronics Department of Kadir Has University.

*To **OMAR** with love...*

LIST of TABLES

LIST of FIGURES

LIST of ABBREVIATIONS

Al_2O_3	....……. Aluminum Oxide
CMOS	……. Complementary Metal Oxide Semiconductor
CVD	……. Chemical Vapor Deposition
DEA	……. Diethanolamine
FoM	……. Figure of Merit
ICDD	……. International Centre for Diffraction Data
ITO	……. Indium Tin Oxide
IZO	……. Indium Zinc Oxide
MoS_2	……. Molybdenum disulfide
PD	..... Photodetector
PLD	..... Pulsed Laser Deposition
PW	……. Pure Water
RF	……. Radio Frequency
SnO_2	……. Tin(iv) oxide
TCO	……. Transparent Conducting Oxide
UV-IR	……. Ultra Violet-Infra red
UV-VIS	……. Ultra Violet-Visible
XRD	……. X-Ray Diffractometer
ZnAc	……. Zinc Acetate dehydrate
ZnO	……...……. Zinc Oxide
ZnO/MoS_2	……. Zinc Oxide / molybdenum disulfid

1. BACKGROUND, OBJECTIVE, STRUCTURE AND ORGANIZATION OF THE THESIS

1.1. INTRODUCTION

Transparent films are basically composed of materials distinguished by their ability to become optically transparent and also high electrically conductive, called Transparent Conductive Oxide, as the name suggests (TCO). Since transparent conductive oxide films are required to be both transparent and conductive, the figure of merit (FoM) value is calculated, which shows the benefit of both of these two values of transmittance and conductivity. Based on these properties thin film is used in optoelectronics and solar cells. The thin film is composed of layers deposited on top of each other at a certain wavelength. It acts as a resistance to the expulsion of charge carriers outside the photocell, which in turn acts as a window that allows the passage of light rays to the layers below. Energy differences are less than visible region wavelength 380 nm to 750 nm. Photons outside this band gap run out, which means that the visible light pass through it. However, photovoltaic application needs a wide band gap to prevent the unwanted absorption of spectrum. In recent years, TCOs are essential in optoelectronics applications due to their unique properties such good conductivity, high transparency in visible region, reflectivity for IR beam and poor light absorption materials (A. Smith *et al*, 1995).

In order to consider the effectiveness of these deposition techniques which include chemical vapor, pulsed laser deposition, sputtering, spray pyrolysis, evaporation, sol-gel dip/spin coating method to get better TCO thin film performance can be maintained.

Most preferred TCO today for optoelectronic applications is indium-doped tinoxide (ITO). ITO, which constitutes the main material of the television screens and all touch screens that we use in daily life, contains Indium that the damages caused by the degradation of indium threaten the health of living things. Despite its convenient optical and electronic properties, rising costs in recent years since the Indium resources is decreasing in the Earth, intensifies research on alternative materials with features that can replace ITO. The high FoM of the Indium Zincoxide (IZO) film deposited at room temperature comparable to that of ITO shows that it is promising for applications in OLEDS, organic solar cells, and flexible electronics. It is not possible to recycle the

indium contained IZO films due to the numerous damages it causes to health. Instead of indium, another additive that can provide the same level of conductivity must be made to Zincoxide (ZnO).

As a semiconductor, ZnO is recognized because at room temperature it has fast transparent properties and efficient for light harvesting that's used in solar cell application, as well as good thermal and mechanical stability. Commonly, thin films of un doped ZnO usually show n-type conduction. In general, semiconductors have a wide band gap and high electron-hole recombination, to solve this a noble metal like Au, Ag or nano-particles like AuPd added (E. Arca *et al*, 2012) (V. De La Garza-Guadarrama *et al*, 2001). ZnO has a broad range of excitons, strong binding force, high strength, high stiffness and larger specific electronics mobility.

At the same time, there are excellent physical and chemical properties of the two-dimensional MoS_2 flake, like big surface to volume ratio, the major band gap approximately starts from 1.2 eV and 2.2 eV is the maximum energy, also it has many active edge and high mobility of electrons in the plane. By regulating film thickness, MoS_2 can achieve tunable electronic / photoelectron performance. Furthermore, MoS_2 has strong chemical stability, also it is not difficult to combine and utilize silicon compatibility with process in CMOS logic products. Short channel effects can be effectively suppressed by ultrathin MoS_2 nanosheets. Nanomaterial components of MoS_2 used in many applications such as batteries of electronic / optoelectronic devices, photocatalysis, lithium-ion devices, and lithium-ion nanomaterials because of these advantages. However only 5.6 percent of the bulk content is absorbed by the monolayer's MoS_2, which significantly restricts its use in photodetector (PD) devices and photocatalysis Haacke (1976). Nano-molybdenum disulfide is commonly combined with other near-atomic-distance semiconductors to create a composite to satisfy these applications. MoS_2 can be considered as another additive instead of indium to ZnO that can provide both the high conductivity and transparency.

The specific objectives of this work were to study the electrical and optical characteristics of ZnO/ MoS_2 transparent conducting thin film. However, when preparing this new TCO film, the important thing is, as for other methods, to distribute the additive material homogeneously in the main material. When MoS_2 additive is made in a small amount (low molar ratio), it cannot form the conductivity mechanism. Because in a very sparse

structure, conductivity electrons cannot be transmitted from end to end. Due to the possible discontinuity in the carrier conduction line, the density of the additive should be optimized. On the other hand, by adding excess MoS_2 to ZnO, it is possible to make the composite material more conductive. In this case, optical transmittance is compromised so that the final material is not TCO. Therefore, it is crucial to determine with which technique, at what stage of the process and how much MoS_2 will be added.

In order to obtain a homogeneous material with desired properties, it is necessary to mix the starting chemical solutions in certain proportions and check whether the particles belonging to different chemicals are homogeneous in the material over and over again. These trials should continue until the best value is found. There are many methods for determining the distribution of particles: SEM, TEM, light scattering (zeta sizer). Although these are extremely costly methods, it is impossible to measure all materials prepared at different concentrations with these methods, as it becomes expensive. Optical method, which is extremely reliable, easy and the cheap, calculates the resonance ratio and normalized width values from the absorption response of the composites according to the wavelength. and then the dispersion rate of the MoS_2 in the composite film is determined. The proper ultra-sonication process has been realized so as to maintain the good dispersion of the MoS_2 inside the ZnO matrix lowering the normalized width and increasing the resonance ratio. The thesis is organized as follows: Chapter 2 introduces the literature review, manufacturing process of TCOs and their applications. Chapter 3 focuses on the experimental methods and characterization techniques of this research. In Chapter 4, the results are given, and the discussion of results takes place. The conclusion section is given later.

2. LITERATURE REVIEW AND TRANSPARENT CONDUCTIVE OXIDES'S MANUFACTURING PROCESS AND APPLICATIONS

2.1. LITRETURE REVIEW

Transparent Conductive Oxides (TCOs) has an important role in a variety of applications, e.g., flat-screen panels, photocatalysts, solar cells, batteries, and computing devices. ITO, known as the best transparent conductive material, contains the living organism enemy indium additive, its mechanical instability and the difficult production process limit the applications of TCO materials (Adedokun, 2018). Various alternatives to overcome these limitations inexpensive and plentiful materials attracted great attention. Among this various materials zinc oxide (ZnO) has emerged as one of the most promising. ZnO has a high optical transparency in the visible region, but low electrical conductivity. In order to improve the electrical properties of ZnO without impairing its unique optical properties, a method of doping with group-III elements (In, Al and Ga) has been tried (Hsu et al., 2018). In Table 2.1, the optical and electrical properties of ZnO doped with different materials are reviewed. Using these values, FoM value was calculated with Haacke's approach which will be given in Chapter 2. The higher the FoM value the better TCOs. According to Table 2.1, the best TCO with the highest FoM value is AgZnO (Silver Nanowire Zinc oxide).

The transparent conductive oxide of Al-ZnO characterize as high transmittance and low resistance in visible region. It is possible to control in the bandgap by doping with Al. ZnO (TCO) used in application that's need high and low resistivity such as solar cell, optical coating. Sputtering, pulsed laser depositions, chemical vapor deposition and chemical spray are used in TCO fabrication.

Table 2.1. The review of various materials doped ZnO transparent conductive oxides with their sheet resistance and transmittance values.

Material	Deposition Method	Sheet Resistance (ohm/sq.)	Transmittance (%)	Figure of Merit (FoM)	Reference
AZO (Aluminum Zinc Oxide)	Sol-gel	148.43	66.23	1.09E-04	Tonny et al, 2018
AgZnO (Silver Nanowire Zinc oxide)	Sol-gel	8	91	4.87E-02	Kim et al, 2013
Ga/ZnO (Gallium Zinc Oxide)	PLD	40.6	90	8.59E-03	Lui et al, 2013
In/ ZnO (Indium Zinc Oxide)	Spray Pyrolysis	32	90	1.09E-02	Ali et al, 2018
In/ ZnO (Indium Zinc Oxide)	PLD	42.3	85	4.65E-03	Lui et al, 2013
F/ZnO (Iron Zinc Oxide)	PLD	24.15	90	1.44E-02	Lui et al, 2013
Si/ZnO (Silicon Zinc Oxide)	PLD	41.33	80	2.60E-03	Lui et al, 2013
Cl/ZnO (Chlorine Zinc Oxide)	CVD	41.9	80	2.56E-03	Jiamprasertboon et al, 2019

To manufacture SnO_2 some elements used as dopant. Dawood *et al.*, show that the propagation of optics is highly related to doping in thin films of indium tin oxide related to free electrons (ITO). These are observed that ITO thin films frequently improve optical transmission with doping levels as conductivity rises. Transmission declines, with light doping declining by around 2 to, for the heavily doped sample of indium tin oxide. Percent in dramatically improves undoped transmission. The decline in doping transmission may be induced by the enhanced dispersion of the photons by doping-generated crystal defects.

Due to the impact of transmission on doping concentration and on deposition, other TCO output properties are often affected" (Dawood *et al*, 2014).

In other hand, Mohagheghi *et al.*, shows the possibility of use Al dopant to produce SnO_2 thin film when spray pyrolysis process applied. They may be categorized in two separate forms, including the physical process and the chemical method, with the various processes available. The physical approach includes deposition processes which based upon on material being evaporated from an available source evaporated. In contrast with techniques for physical deposition, chemical methods provide several advantages, for example, cost, flexibility and simple control of composition and homogenization in conjunction without vacuum in the deposition chamber. In chemical deposition technique, the researchers are responsible for decision-making dependent on considerations such as expense, compliance with materials to be deposited, easily controlled deposition speed, efficiency with temperatures ranging, and the quantity of materials to be deposited in many of the deposition technologies that demonstrate positive results. The sol-gel spin coating method is one of these methods (Mohagheghi *et al.*,2004).

The annealing effects of CuS, CuZnS and ZnS thin films on structural, electrical and optical properties were investigated by (Yildirim *et al.*), reach that annealing seems to be the most suitable thermal process to manufacture TCO thin film. Because the increasing in annealing temperature make the annealing film has resistance higher than grown film also minimize the optical band gap. Instead of strengthening it, hardening and tempering will disorganize the crystal further. Annealing requires heating a substance past its recrystallization temperature, holding an acceptable temperature to be transformed to ample time and then to gradually refried cold. During the annealing process, atoms pass through crystal structure and reduce the dislocations, which is cause to several changes softness and hardness of the crystal. The volume of crystallinity or particles of thin film by using thermal annealing does not change. To increase the conductivity, the contextual ads of oxygen is reduced. Also, the rising of annealing and the temperature of heat treatment at atmospheric reduction rising the conductivity. By reducing oxygen interstitials, the increase in conductivity is achieved. In this way, the physical contact

enhancement increases the conductivity when the temperature of annealing at high rates (Yildirim *et al.*,2009).

Kim *et al.*, in another study of the sol-gel spin-coating process, deposited thin films of Al-coated zinc oxide on quartz substrates using the sol-gel spin-coating technique. As a starting material, zinc acetate dehydrates [Zn $(CH_3COO)_2 \cdot 2H_2O$] was used the stabilizer and solvent were monoethanolamine [C_2H_7NO] and 2-methoxyethano [$CH_3OCH_2CH_2OH$]. Aluminum nitrate was the dopant source [Al $(NO_3)^2 \cdot 9H_2O$]. In the starting solution, the molar dopant ratio was varied to give a ratio of 1-3 percent to [Al:Zn]. The resulting solution was stirred. For 24 hours. The quartz substrate was heated at 300^{o}C for 10 min. So, the solvent is evaporated, and the organic waste is removed. Solvent solution was lowered for deposition, at 3000 rpm for 20 sec. the solvent was rotated. Until repeating the spin coating and pre-heating process five times, to avoid fractures, AZO films have been cooled at 5^{o}C per minute. In a furnace for ambient air at 550^{o}C, the AZO-thin films obtained were then heated for 60 minutes (Kim *et al.*, 2012).

Jafan *et al.*, use sol-gel process to manufactured ITO thin film, ($In(NO_3)_3H_2O$, 99.99 %) and inorganic component ($SnCl_4$, 98 %) are used, as a polymerizing agent and binding material, polyvinyl alcohol, double-distilled water, absolute ethanol and acetyl acetone (98%) as solvents and hydrochloric acid (37%) as a solvent dispersant (Jafan *et al*, 2014).

Lu et al found that the optical absorption spectrum evaluation of $E_{g\ op}$ was primarily related to intensity of carriers and thus essential to aluminum content. Burstein-Moss described that $ne \leq 4.2 \times 10^{19}$ cm^{-3}, the optical gap increased with the electron concentration; unexpectedly decreased in energy gap occurred at $5.4{-}8.4 \times 10^{19}$ cm^{-3}, compatible with Mott SMT criteria. (Lu *et al*, 2007).

Park, Agura *et al*., found that on low resistivity two types of films were prepared GZO&AZO by using PLD. ZnO thin film record good resistance between 5-10cm, also ZnO thin film that prepared by using PLD gives best conductivity in comparison with other process. Due to high cost and satiability problems eliminate the wide use of this process (Park *et al*, 2006).

Luo et al., developed flexible process to film deposition. The principle of this process mixes between a non-aqueous sol gel by using the microwave and coating dip. Although, it is given high resistivity, but by improving each step-in sol-gel process included production of the nano particles, dispersion and thin film treatment and annealing, the production of thin film will improve (Lui *et al*, 2014).

Thin films of Ga-doped ZnO were prepared by Shin et al. (GZO) using RF magnetron sputtering on glass and Al_2O_3 (0001). He found that in GZO there is visible grains on the substrates at the same condition of process. In the GZO film on the Al_2O_3 substrate, however it is difficult to distinguish individual grains. Compared with epitaxially grown GZO films on Al_2O_3 substrates, the superior crystal content of the epitaxially grown GZO films. Better electrical characteristics have been provided by polycrystalline GZO films on glass substrates.

The film crystallinity and stoichiometry, resistivity, and transmittance curves of Si-doped ZnO thin films deposited both on glass and PET substrates were calculated by Clatot *et al*. Their findings have verified that electrical and optical properties are highly dependent on the existence of the substrate. Hydroxylation of the surface vacancies, interstitials are studied theoretically and experimentally. Extrinsic doping and other electronics properties are studied for ZnO surface (Clatot *et al*., 2011).

2.2. TCO THIN FILM APPLICATIONS

The manufacturing of thin film has a broad variety uses, as its architectures start from basic single coating to complicated configurations of hundred or more layers which is called multiple dielectric coating. These uses involve the manufacturing of optical modules (Alam and Cameron, 2000), that greatly decrease the surface reflectivity of the optical object, such as polarizers, interference splitters, and anti-reflection coatings (Mokhtar *et al*, 2014).

2.3. TCO THIN FILM PROPERTIES

2.3.1. Electrical PROPERTIES

This range of materials the electric performance is a significant feature. TCO films are mostly made from asymmetric scaling, due to their high conductivity. The donors of oxygen free electrons the over metals ions are supplies. Those donor sites can be easily identified through a chemical reduction. Carrier agility is one of the key drivers of TCO films' conductivity. The mobility of the carriers in the polycrystalline film depends on the way the imperfection of the grille is spread. The electrical conductivity of TCOs is somewhat inverse to their optical transmission (Adedokun, 2018).

2.3.2. Optical Properties

When the electromagnetic radiation interacts with visible light, the visible region of electromagnetic beam extent from 0.39-0.77μm which is defined as optical properties. As a solar-powered semiconductor, tin oxide thin film is helpful to clarify the behavior of the thin film by solar electromagnetic radiation. Understanding refractive index ‘n’ which is refer to the light speed before and after passing through a medium. Another important factor called extinction coefficient ‘k’ which is refer to how the force of the absorbed light in the medium at a given wavelength. When a light enters the surface it is scattered to three parts: one is reflected on the surface which the transport medium absorbs another part, and the last one is carried out of the surface (Manoj *et* al, 2007). There is no medium in which spectral absorption does not occur, but the absorption rate varies from one medium to another based on several factors.

To study thin film; reflection, absorption and transmission are the most important properties that help to know the behavior of the materials and mediums when it is attract with the light.

2.3.2.1. Reflectance

The ratio between the power of the reflected light to the power of the incoming light is called reflection *R.* Reflectance is a component of the response of the electronic structure of the material to the electromagnetic field of light, and is in general a function of the frequency, or wavelength, of the light, its polarization, and the angle of incidence.

2.3.2.2. Absorbance

A material's absorbance A is determined by the intensity of radiation, I, that absorbed by a material to the quantity of the incident intensity of radiation, I_O. When the light beam enters the material some of it absorbed by the material, the amount absorbed light determined. The value of the absorbed light depends on the thickness, t. The fraction energy value is the same at each thin film layer and reducing thickness of thin film also reducing wave's fraction energy. This change in the value of wave's energy through thin film called absorption coefficient α.

$$\alpha = 2.303\ A / t \quad \text{…..……..} \quad (1)$$

2.3.2.3. Transmittance

The amount of radiant power that transmitted through a medium to the amount of incident power called as transmittance T.

$$T = I/I_O \quad \text{...…….} \quad (2)$$

Transmittance T is < 1, as a result of that the incident light intensity is biggest than the intensity of transmitted light.

$$\alpha = \ln (1/T)\ / t \quad \text{..……...……...} \quad (3)$$

2.4. FACTORS THAT AFFECT ON THE PROPERTIES OF THIN FILM

The method of transforming TCOs into special materials includes deposition processes which include variables such as deposition time, heat-treating temperature, atmospheric conditions, deposition apparatus and the source of materials being used in these processes. All these factors influence the outcomes of the deposition and need endless research on deposition techniques. The advantages and drawbacks of deposited TCOs are analyzed by a process called characterization. Optical characterizations using the UV-IR Spectroscopy; morphology characterization by using four-point probe method; diffraction of X-Ray characterizations structurally, atomic force microscopy, scanning electron microscopy, and electron transmission microscopy are some of the characterization methods being used (Stoica *et* al, 2000), (Adnan *et* al, 2010).

2.4.1. Nature of Substrate

The substrate nature is a very important factor in thin film manufacturing process. Materials like plastic, quartz or metals are coated. Thickness, side of substrate and temperature have an essential effect on the efficiency of transparence conductivity film. For example, to produce glass thin film which is TCO deposited substrate. The additional advantage to this glass substrate is blocked the IR wavelength (1 μm for silicates) and transformed into heat on the glass sheet, besides the support on which oxide may expand. Layer thickness also differs with the wavelength of the incident light, which influences the image optical properties (Adedokun *et al*, 2018).

2.4.2. Doping Concentration

The photo transmittance of thin films ITO increased with increasing the doping concentration and the conductivity. In comparison with the output of undoped transmittance. The adopt addition may be effect on TCO regardless the type of substance, deposition process or TCO. The increasing in photon dispersion that caused by crystal default of dopant will decrease the transmittance. So, the type of dispersion process and the concentration of dopant effect on the TCO properties and transmission (Kumara *et al*, 2014).

2.4.3. Deposition Techniques

The materials required for the manufacture of thin films are selected according to the application for which they are used. The method of deposition is also determined according to the intent of the thin film for example if it is required to study the electrical properties, the membrane is deposited by the sol gel method, and if the application is chemical, the chemical vapor method is used.

Available deposition processes can be classified into two types: physical and chemical. The physical process is based on evaporation of the source materials. While the chemical method is based on the use of the physical properties of a substance. The chemical method is preferred over physical due to the simple cost and ease of homogeneity control. The process of testing the thin film preparation method is studied based on several factors including cost, control method, temperature and material volume (Liu *et al*, 2013).

2.4.4. Heat Treatment

Deposition process of thin film manufacturing accompanied by defects in film crystal which due to change the properties of the film. To remove this defect, the species structural is heated at the same temperature for specific time and after that cooling it in a sequence by heating treatment these defects will fix. This process also makes the physical morphology strong and expand the application that use in it. Atoms must be daily recombination which due to get new specific properties in a good shape. About (300^{o} C) all process needs acceptable high temperature to produce high conductivity thin film. These conditions may be suitable for other applications like, solar cell hetero-junction, optoelectrical devices for scalable electro-optical devices, hetero-junction solar cells and amorphous silicon-based photovoltaic devices which is failed at high temperature (Liu *et al*, 2013).

2.4.5. Coating Layers

Film's thickness is affected by coating layers' amount. A comparatively higher carrier concentration is included in the thicker layer of coated film, mobility of the carriers and film crack happened as a result of high cumulative internal presser. As several TCOs, before a certain critical thickness is reached, electrical resistivity typically decreases with increased thickness. This pattern often follows other features like structural and optical properties, modifying the reaction direction at a crucial thickness to adjust film thickness.

2.5. THE FIGURE OF MERIT CALCULATION

To evaluate the quality of TCOs, researchers use the concept of figure of merit (FoM). FoM gives a numerical value from the two most important parameters for a TCO: transmittance (T) and sheet resistance (Rs). It is therefore possible to compare the quality of different materials using the same FoM definition. Haacke defined the figure of merit as (Haacke, 1976)

$$FoM = T^{10}/Rs \qquad (4)$$

Or used FOMs are Fraser &Cook (T/Rs). In both definitions, T refers to transmittance and Rs to the sheet resistance. Cisneros-Contreras *et al*., found that FOM Fraser & Cook

exhibits a higher resolution than FOM Haacke. However, FOM Haacke surpasses FoM Fraser & Cook in the evaluation of transparent conductor materials. The latter because in FOM Haacke there is an implicit power function between T and Rs that allows a balanced treatment of T value against the value of Rs.

2.6. SOL-GEL METHOD

This method defined as the creation a network of oxide by the polycondensing. The synthetic precursor fluid reactions. The concept behind the synthesis will be to melt the compound into a solvent in order to return it in a controlled manner. The route which typically leads to small, sintering particles prevents co-precipitation problems as well. Products of a number of types, including porous surfaces, thin textiles, thick powders and thin films are generated using sol-gel synthesis. According to the simple monitoring of the covering step from a drop of solvent, followed by heat processing, the technology is suitable for extensive applications. The sol-gel route offers some advantages in compared to other methods, the sol-gel route provides certain benefits in contrast with other approaches including the ability of deposit over specific substrates simpler doping level regulation, very cheap starting materials and easy equipment. In general, this manufacturing approach would be cost-effective as well as makes the deposition of thin films on more than area. Sol-gel has become a preferred technology which controls a range of characteristics, such as stoichiometric, porosity, crystallinities and morphology. Deposition of this process requires phases such as mixture, gelation, ageing, drying and sintering are required. The solvent is then filled on a substrate with a dip-coating or spin-coating for the formation of a thin film. The solvent was further covered with dip-coating or spin-coating on a layer in order to achieve a thin film. Although dip coating gives the bonus utilization all layer sides, the process of spin-coating process seems easier and low cost.

2.7. UV-Vis SPECTROMETER

UV-Visible spectrometer considered a useful method offer unique methods to determine the exact and semi exact quantities in species analysis. The UV-Vis spectrum generates from transitions between energy level to absorption light of the sample. The ideal

spectrum of UV beams is a graph of wavelength to the absorption intensity and characterized by two factors: the maximum value of absorption and intensity.

Beer-Lambert's law expresses the relation between absorption, concentration and the path length to the species that absorbed which is considered the base of analytic quantitative selections. Some of factors may do not surrender to the law such as pH or the concentration of the electrodes or wavelength.

There are five major components of UV-Vis spectroscopy:

- Source of radiation: such as deuterium lamp for UV and tungsten for visible region.
- Monochromator or using filters for visible region as low-cost option to select wavelength.
- Sample holder.
- Detector by using phototube or diode.
- Signal processing.

These components inter in spectroscopy manufacturing in three types, diode spectrometer single and double beam spectrometer.

The UV-Vis spectrometry uses in many applications such as:

- To detect the ingredients of solution and measure the concentration of each one.
- Also, it used to identify of molecule in organic compound.
- To detect the presence of unsaturation in the molecule.

2.8. X-RAY DIFFRACTOMETER

X-ray diffraction (XRD) is the technique that reveals structural information, such as crystal structure, crystallite size, chemical composition, and strain. It can be used to analyze thin films and powders. The only condition to use the XRD method is that the material has a crystalline structure. A crystalline material consists of a highly ordered microscopic structure, forming a regular array of atoms. It is possible to form a crystalline structure inside the material by changing the medium's pressure or temperature. When x-rays are applied on the material, the atoms of the material which aligned onto these crystalline structure (like atoms placed at the corners of the cube), atoms scatter the x-rays. Since the x-rays are waves of electromagnetic radiation, some of these waves cancel

one another out in most directions and some of them are strengthen other waves in a few specific directions. This relationship is determined by Bragg's law:

$$n \lambda = 2 d \sin \theta \quad \text{.....(5)}$$

Here d is the spacing between crystal planes, θ is the incident angle, n is the integer, and λ is the wavelength of the x-rays (Bragg, Bragg, 1913).

To calculate the crystallite size, Debye–Scherrer's equation is used (Scherrer, 1918):

$$\beta_{size} = K \lambda / L \cos \theta \quad \text{.....(6)}$$

where β_{size} is the peak width at half-maxima, K is the constant of X-ray source and L is the crystallite size.

The formula of Debye–Scherrer discusses just the effect of crystallite size on the XRD peak broadening, but it explains nothing about the lattice microstructures, i.e. the intrinsic strain that is formed in the nanocrystals due to the point defect, grain boundary, triple junction, and stacking defects (Nath et al, 2019). Broadening of XRD peak occurs due to the size and microstrain of the nanocrystals and the total broadening can be written as,

$$\beta_{hkl} = \beta_{size} + \beta_{strain} \text{.....(7)}$$

The intrinsic strain effects the physical broadening of the XRD profile and the strain induced peak broadening can be expressed as,

$$\beta_{strain} = 4\varepsilon \tan\theta \text{.....(8)}$$

where $\boldsymbol{\varepsilon}$ is the intrinsic strain of the material. Average particle size (the crystallite size) and strain can be calculated using Williamson-Hall equation (Williamson and Hall, 1953):

$$\beta_{hkl} = K \lambda / L \cos\theta + 4\varepsilon \tan\theta \text{.....(9)}$$

2.9 FOUR-POINT PROB METHOD

The sheet resistance (Rs) represents an intrinsic material property that is a common electrical property used to characterize conductive films. It is a measure of the lateral resistance through a thin square of material. It can be measured directly using a four-point probe method.

Sheet resistance (Rs) is commonly defined as the resistivity (ρ) of a material divided by its thickness (t):

$$Rs = \rho / t \quad \text{.....(7)}$$

The units of sheet resistance must be Ohms (Ω) according to this equation, however, Ohms per square (Ω/□) is the unit of sheet resistance used since it represents the resistance between opposite sides of a square of a material (rather than bulk resistance).

A four-point probe consists of four electrical probes in a line, with equal spacing between each of the probes as shown in Figure 2.1. The four probes are in contact with the surface of the film. The potential difference (ΔV) is applied between probes 2 and 3, and the current (*I*) is measured flows from probe 1 to probe 4. The sheet resistance is calculated using the equation below:

$$Rs = \pi \Delta V / I \ln(2) \quad \text{.....(8)}$$

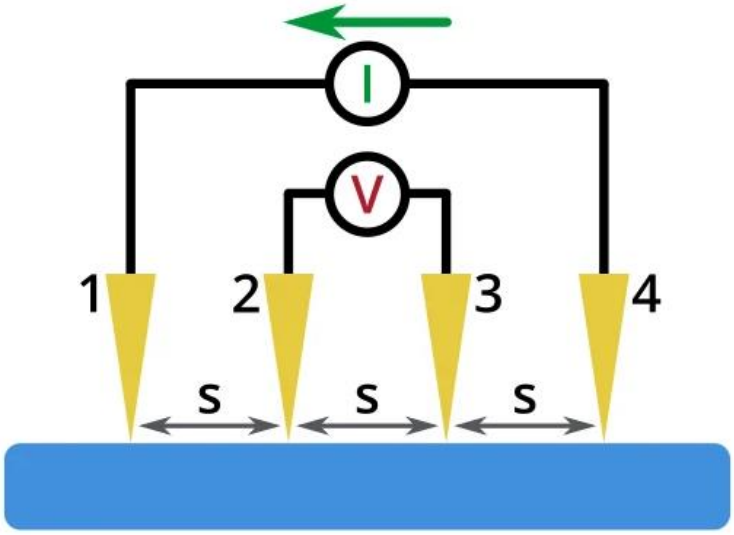

Figure 2.1. The working scheme of four-point probe method.

3. EXPERIMENTAL METHODS

3.1. EXPERIMENTAL PROCESS

ZnO/MoS_2 composite films were prepared using the sol-gel method. Zinc acetates dehydrate (ZnAc) is a precursor material in order to obtain ZnO structure. Diethanolamine (DEA), which is a surface-active material, was used to accelerate dissolving. Pure water (PW) was added for hydrolysis reactions. The sol was prepared by dissolving ZnAc in isopropanol (2propanol) using magnetic stirring and hot-plate at 60°C. After all precursor material had dissolved, Molybdenum disulfide (MoS_2) was added to the solution. A homogeneous and stable sol was prepared by dissolving MoS_2. Then, DEA was added, and a vigorous stirring process was performed under ultrasonic conditions with a frequency of 1kHz. After the condensation, precursor solution was hydrolyzed using ZnAc:2propanol:DEA:PW:MoS_2 with a volume ratio of 0.4:3.5:0.2:0.25: (0, 1, 2, 3, 4 mg). Figure 3.1 illustrates ZnO solutions with MoS_2 amounts of 0 mg, 2 mg, and 4 mg. As expected, the ZnO film containing 2 mg MoS_2 has a lighter color than the ZnO film containing 4 mg MoS_2. The undoped film has a lighter appearance. Hence, as the amount of MoS_2 in the solution increases, the darker the color indicates that the MoS_2 is well dispersed in ZnO. In addition, it is seen in Figure 3.2 that MoS_2 in the solution precipitates when ultrasonic treatment is not applied while preparing the solution.

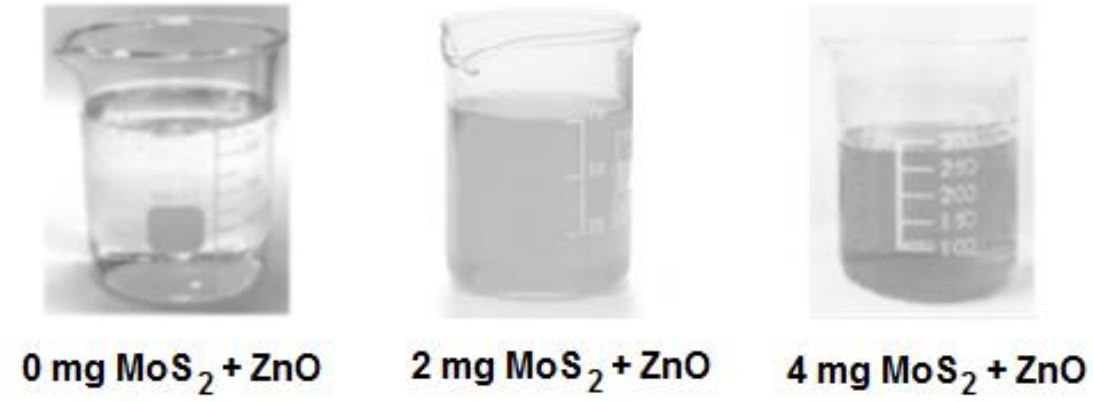

Figure 3.1. Photographs of ZnO solutions prepared in various MoS_2 amounts in beakers.

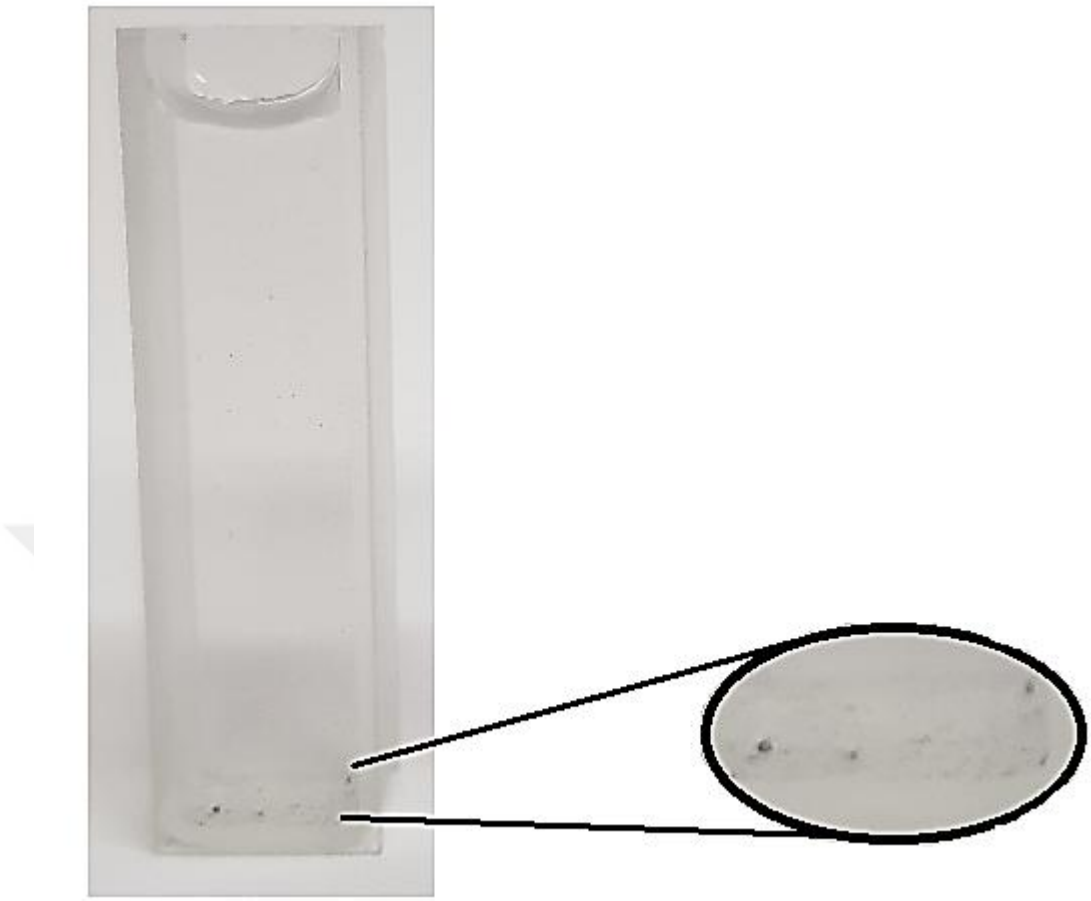

Figure 3.2. The photo of ZnO solution with MoS_2 amount of 1 mg prepared without ultrasonic treatment. **Inset:** MoS_2 precipitation in the solution.

Corning 2947 glasses were cut with a diamond knife to obtain squares with a side of 1 cm. After all the cut glasses were washed with glass detergent and cleaned with ethanol, they were cleaned of stains on them in an ultrasonic bath and dried. The obtained solution was deposited on Corning 2947 glass substrates by spin-coating deposition (1000 rpm/30 s). After coating, ZnO/MoS_2 composite films were immediately placed in a microprocessor-controlled (CWF 1100) furnace which was already heated at 250°C. The first layer on the substrate was formed. The coating and annealing processes were repeated four times to achieve the desired high conductivity of the film (Figure 3.3). The films were taken out of the furnace at the end of the last annealing process at 450°C and left at room temperature.

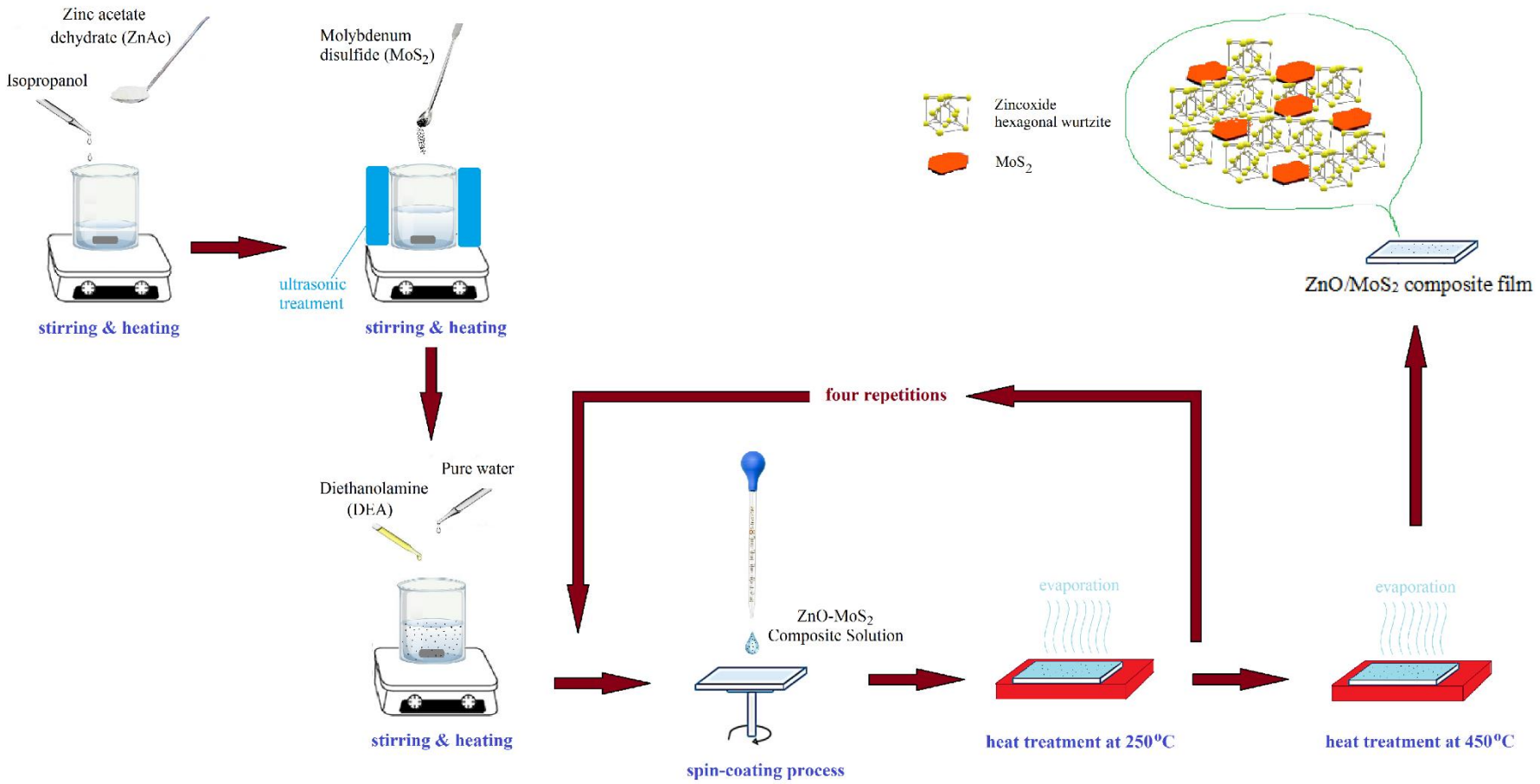

Figure 3.3. Preparation of coatings by sol-gel method

3.2. CHARACTERIZATION

The structure of composite films deposited on Corning-2947 substrates was characterized by X-ray Diffractometer (XRD, Philips PW-1800, Cu-Kα radiation). The XRD spectra of the films were recorded by scanning 2θ in the range 20–50°. To match the XRD peaks with the proper Miller indices, International Centre for Diffraction Data (ICDD) and Materials Project online platform were used. UV-vis spectroscopic analysis of films was performed using UV-visible absorption spectrophotometer (Perkin–Elmer Lambda 900 with Labsphere integrating software) in the spectral range of 190-1100 nm wavelengths. The calculations of under the curve area, full-width of half maximum of the absorbance data were performed by Origin 8.0 Software focusing the absorbance data in the range of 190-400 nm wavelengths. To determine the sheet resistance of the obtained films in square geometry, the four-point probe method was used.

We use the methods that observe the parts of the curve. The dispersion measured by parts or sub-branches using UV-Vis spectroscopy to recognize the solution dispersion. To improve the dispersion scales which is based on identifying UV-Vis to the reorganization of ZnO dispersion solution. The background area was undergoing comparison with the resonant ratio and the normalized width.

3.3. DISPERSION CALCULATION THEORY

First, smoothing of the curve was realized by using Origin 8.0 (Figure 3.3.1). After that the amount of area for resonant band was calculated by using integration property in Origin 8.0 (Figure 3.3.2).

When calculating the non-resonant background area, the maximum part of the absorbance curve is taken. One can need to calculate the area of that part. Values on either side of the maximum curve for the data, the wavelength values are that corresponds to the absorbance value are taken. The part with these values forms a line. After that, the equation for this line is found, and the area under this line is calculated. If the area below the line (the non-resonant background) is subtracted from the area under the maximum curve, the area of resonant band is found (Figure 3.3.3):

Resonance ratio = (area of resonant band) / (area of non-resonant background) ……..(9)

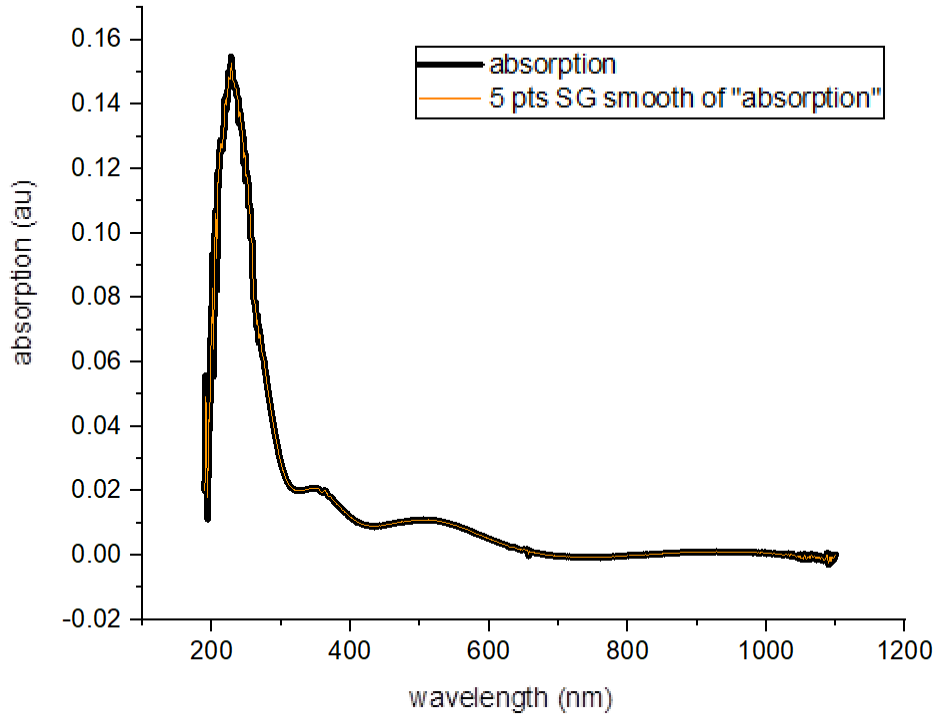

Figure 3.3.1. The absorption curve of composite after smoothing.

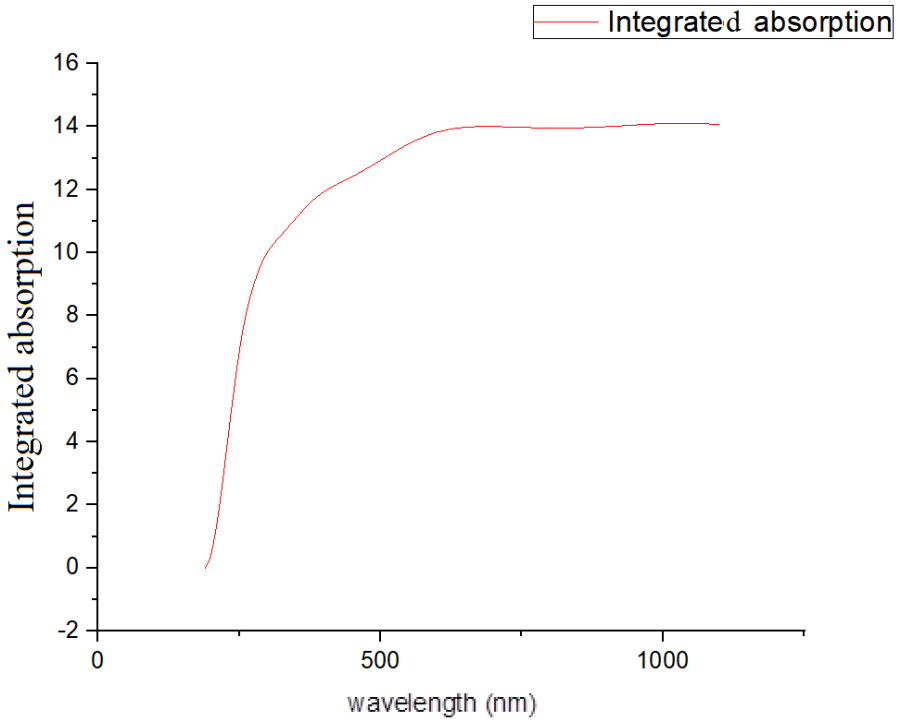

Figure 3.3.2. Integration of absorption –wavelength curve yields the resonance area of absorption.

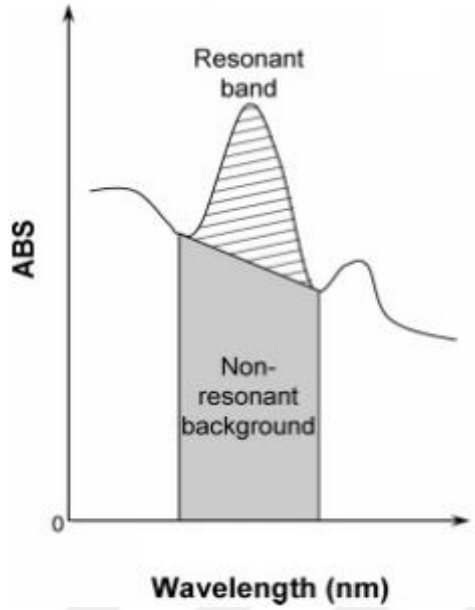

Figure 3.3.3. The calculation method of resonance band and non-resonance background (Tan *et.al*, 2005).

Also, the normalized width at half height of the peak can be found by taking the ratio of the width of resonant band and height of resonant band. The normalized width of absorbance curve is determined from the following formula:

Normalized width = (width of resonant band) / (height of resonant band) …….(10)

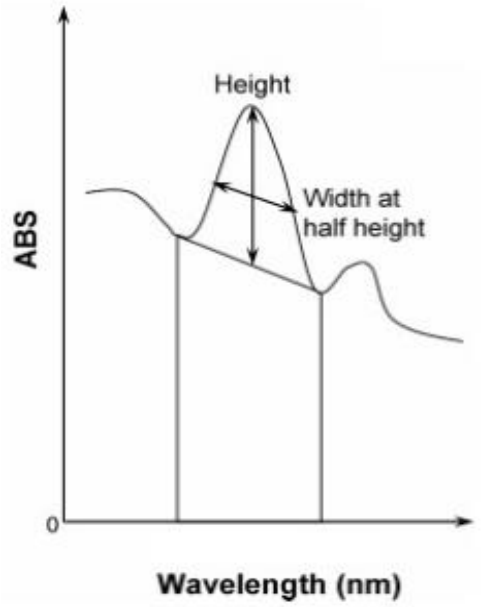

Figure 3.3.4. The definition scheme of width and height of resonant band in order to calculate the normalized width of dispersion (Tan *et.al*, 2005).

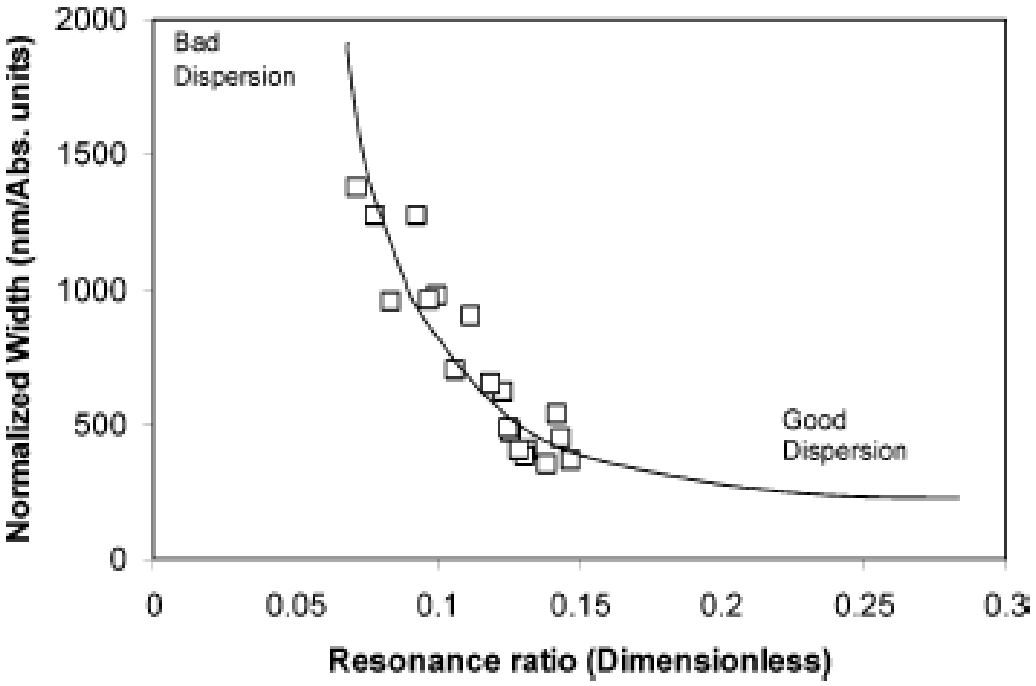

Figure 3.3.5. Combined resonance ratio and normalized width of UV-vis Spectra. The most effective dispersion exhibits a low width ratio and high resonance ratio. (Tan *et.al*, 2005).

4. RESULTS AND DISCUSSION

4.1. OPTICAL STUDIES AND DISPERSIBILITY

The importance of the dispersion makes these properties as intensive properties which is not changed with road path/ wavelength.

The use of different concentration shows different effects on dispersion factors, which shows that the decreasing in the peak width with increasing time of the sonication, which means that the resonance sheet become more sharp and high and therefore offer increasing in nano particles. Table 4.1 summarize the calculations from the dispersion theory as mentioned in Chapter 3. As observed in Table 4.1, the increase in doping amount results in the increase in the area of resonant band until the amount of 4 mg. In addition, the resonance ratio of the samples is decreasing after that it is increasing with an increase in doping amount. The best dispersion can be obtained for the lowest normalized width and the highest resonance ratio. To find out the best dispersion, new figure has to be plotted for these values. Figure 4.1. illustrates the normalized width versus the resonance ratio curve. The most effective dispersion which exhibits a low width ratio and high resonance ratio is for doping amount of 4 mg.

Table 4.1. The calculations of resonant ratio and normalized width of ZnO/MoS_2 transparent oxides

Sample with doping amount of MoS_2 in mg	Area of resonant band	Area of nonresonant background	Resonance ratio	Width of resonant band (nm)	Height of resonant band (au)	Normalized width (nm/au)
0	14.0664	2.7493	5.1164	113	0.1546	730.9185
1	90.7485	20.12	4.5104	160	0.1714	933.2439
2	101.9256	21.6664	4.7043	160	0.2025	790.0064
3	116.8828	18.3885	6.3563	86	0.2250	382.1859
4	104.6548	10.0995	10.3624	50	0.2354	212.4104

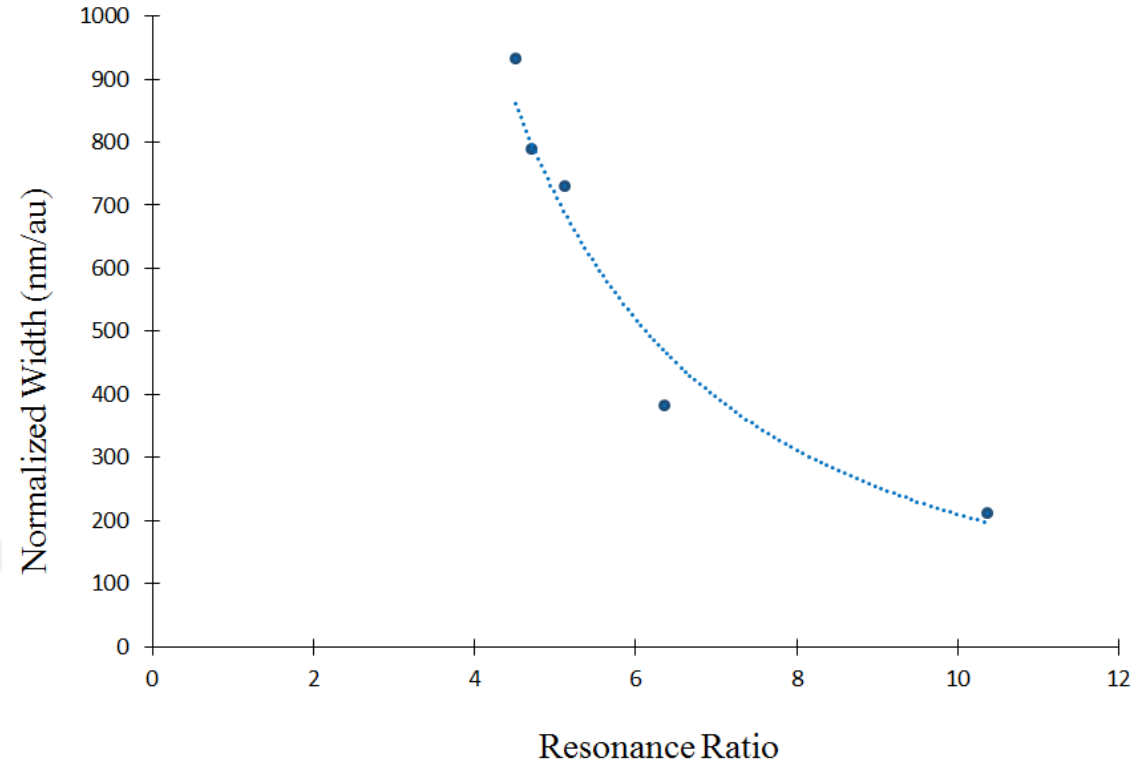

Figure 4.1. The normalized width versus resonance ratio curve to determine the best dispersed film.

Figures 4.2-6 illustrates the normalized absorption curves of ZnO films with various MoS_2 doping amounts. The absorption response of the non-doping film exhibits the same characteristic peak of ZnO near 240 nm as seen in Figure 4.2. This peak shifts to longer wavelengths with the increase in the doping amount of MoS_2. Because, MoS_2 has a characteristic peak at another wavelength (around 500 nm) which is longer than the peak of ZnO. The shift is getting larger according to the increase in doping amount. Finally, in Figure 4.4, it is obvious to see more than one peak in the absorption response of composite films. Compared absorption intensities manifest that the increase in doping amount of MoS_2 promotes the opacity, which leads to the increase in the absorbance intensity as expected. It is a proof of the well-dispersed composite films.

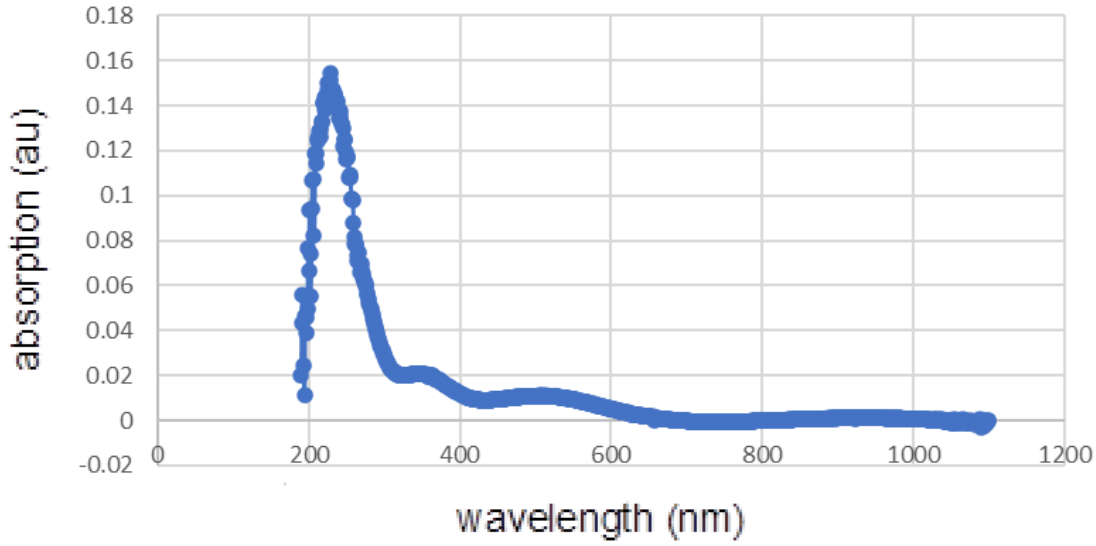

Figure 4.2. The absorption of ZnO films without doping.

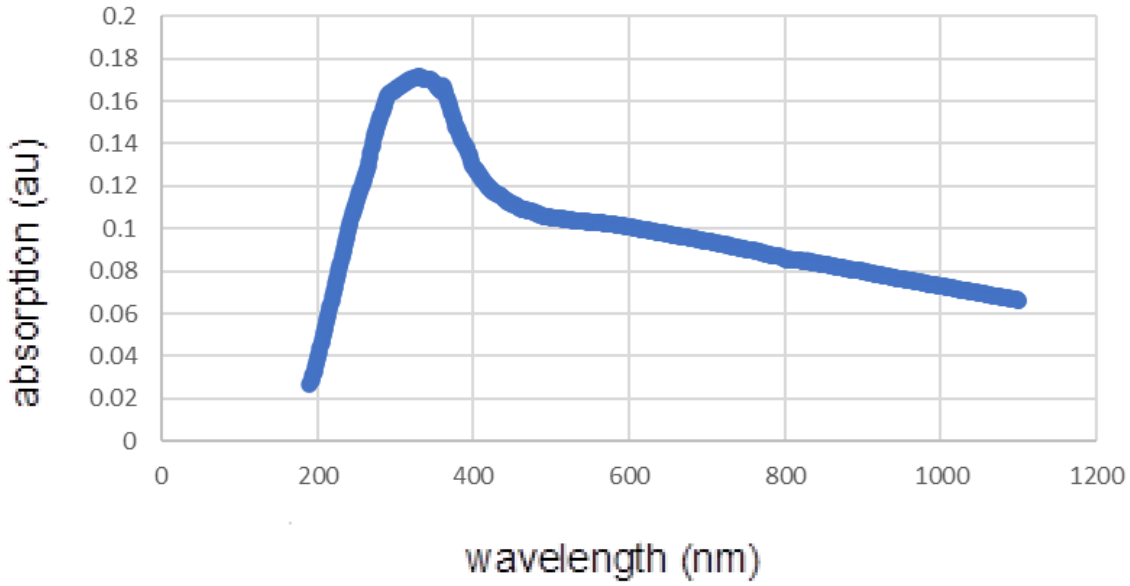

Figure 4.3. The absorption of ZnO films with MoS_2 doping amount of 1 mg.

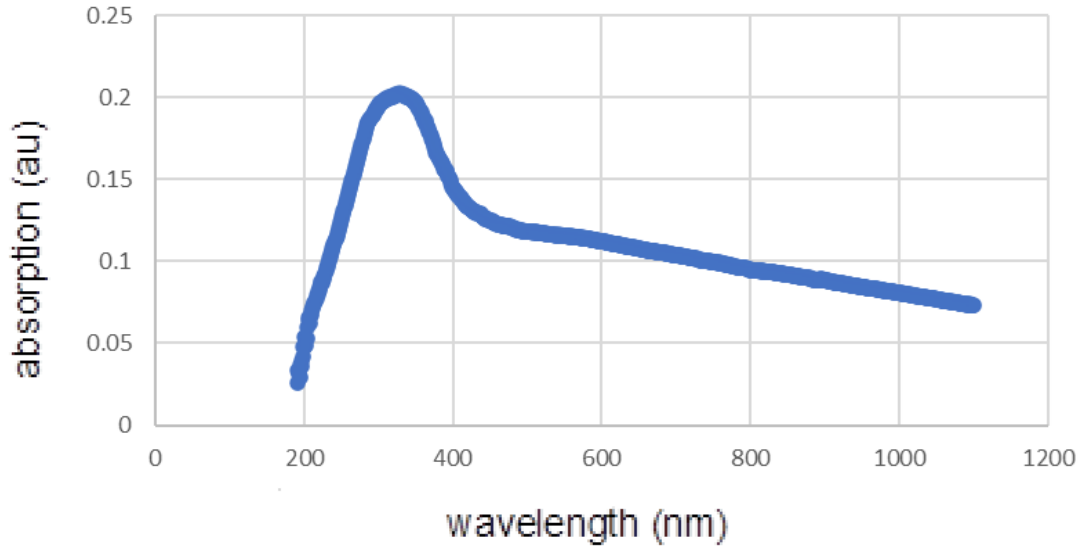

Figure 4.4. The absorption of ZnO films with MoS_2 doping amount of 2 mg.

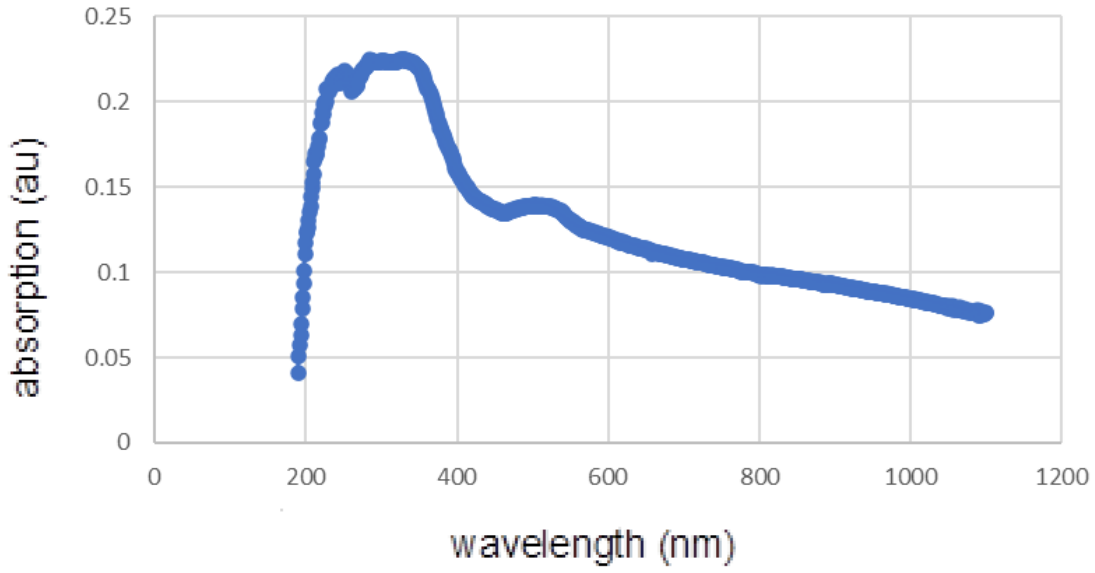

Figure 4.5. The absorption of ZnO films with MoS_2 doping amount of 3 mg.

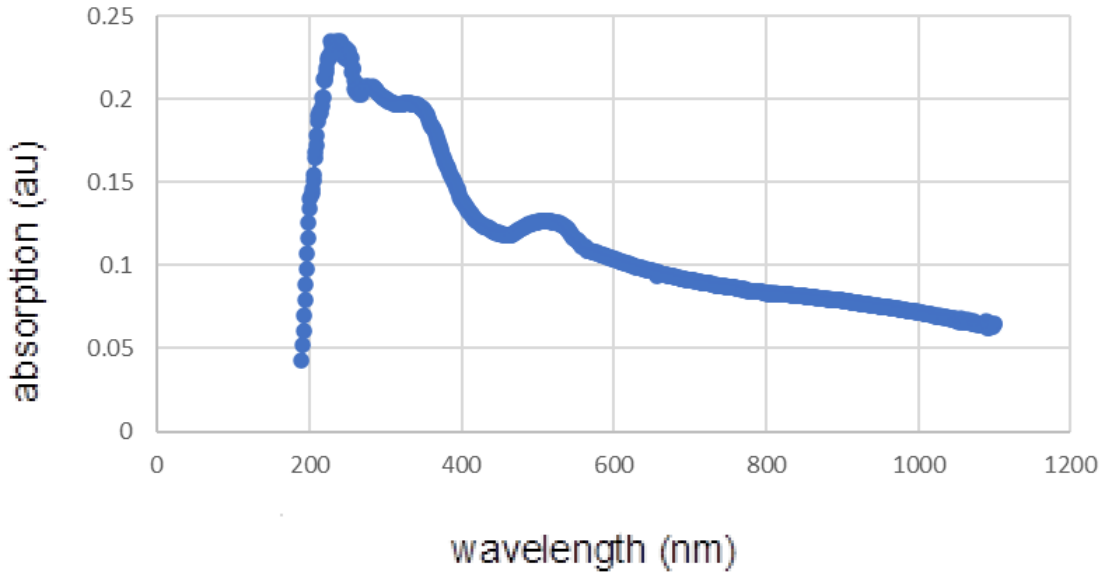

Figure 4.6. The absorption of ZnO with MoS_2 doping amount of 4 mg.

Figure 4.7 depicts the transmittance graphs of ZnO films with various MoS_2 doping amounts. It is obvious to see that the transmittance value of the films is decreasing with the MoS_2 doping amount. The graphs can be divided into two regions as short wavelength region (Region I) and long wavelength region (Region II). The optical properties of the composite material differ in these two regions. It appears that the opacity of the film is promoted by the increase in the amount of MoS_2. Whereas the composite films give a low-transmission response to the ultraviolet light in Region I, it is observed that the films remarkably absorb UV light with long wavelength. In Region II, all composite materials are highly translucent. The fact that they have high transmittance percentage (the range between 85% and 96%) in the visible region is in agreement with the photographs taken just after the gelation of the solutions in the beakers (Figure 3.1). As expected, the ZnO film containing 2 mg MoS_2 has a lighter color than the ZnO film containing 4 mg MoS_2. The undoped film has a lighter appearance. This result confirms the structural homogeneity just as in Figure 3.1. And also, the transmittance curves of the composites in Region II (Figure 4.7) are in agreement with the observations from Figure 3.1. Lower transmittance observed for MoS_2 doping amount of 4 mg can be attributed to the agglomeration of ZnO particles for higher amount of MoS_2.

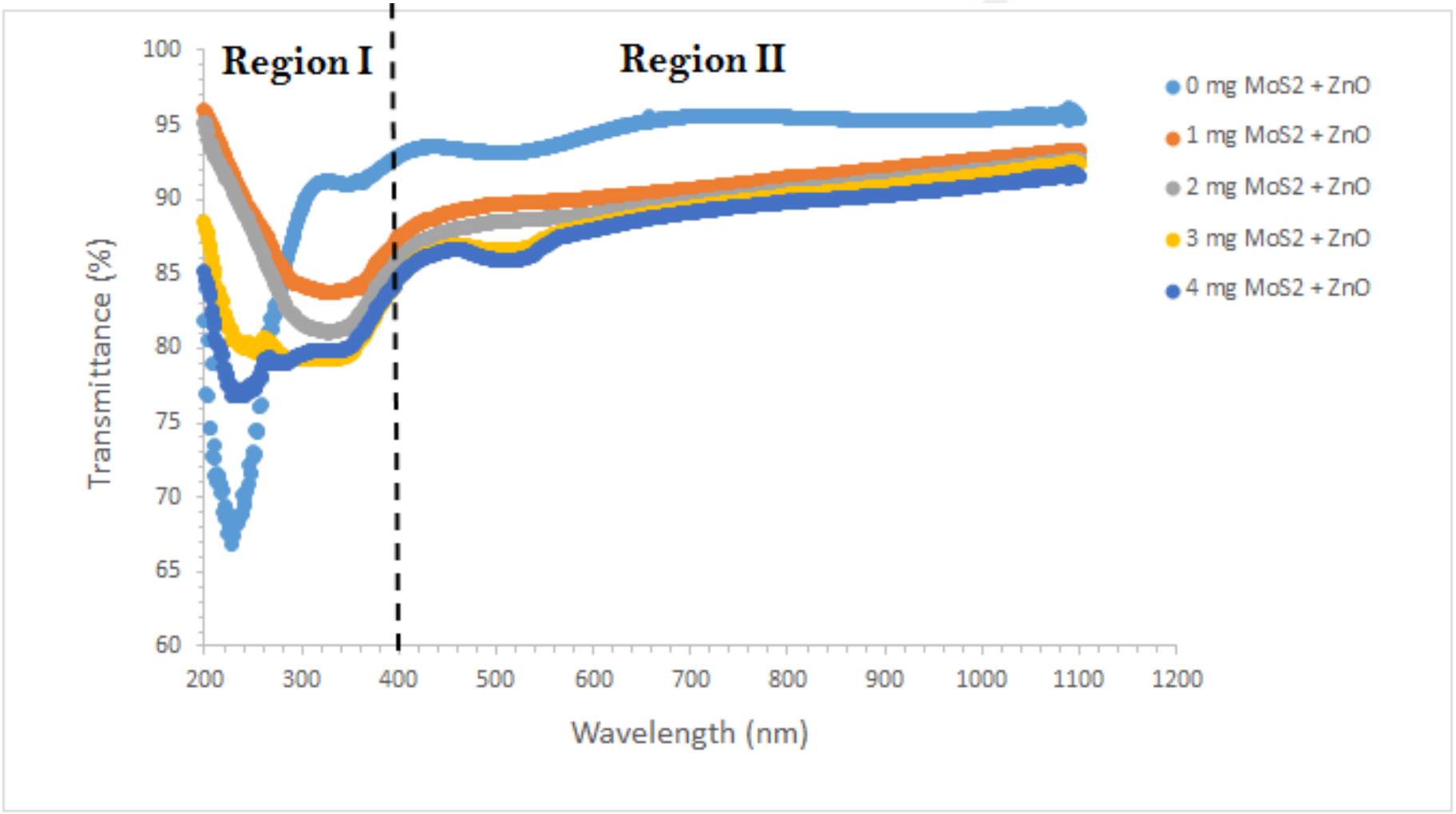

Figure 4.7. The transmittance of ZnO films with various MoS_2 doping amounts.

4.2. STRUCTRAL STUDIES

The XRD plot of ZnO undoped film is shown in Figures 4.8(b). It is seen that the undoped film has hexagonal wurtzite structure (ICDD: 36-451) as seen in Figure 4.8 (a).

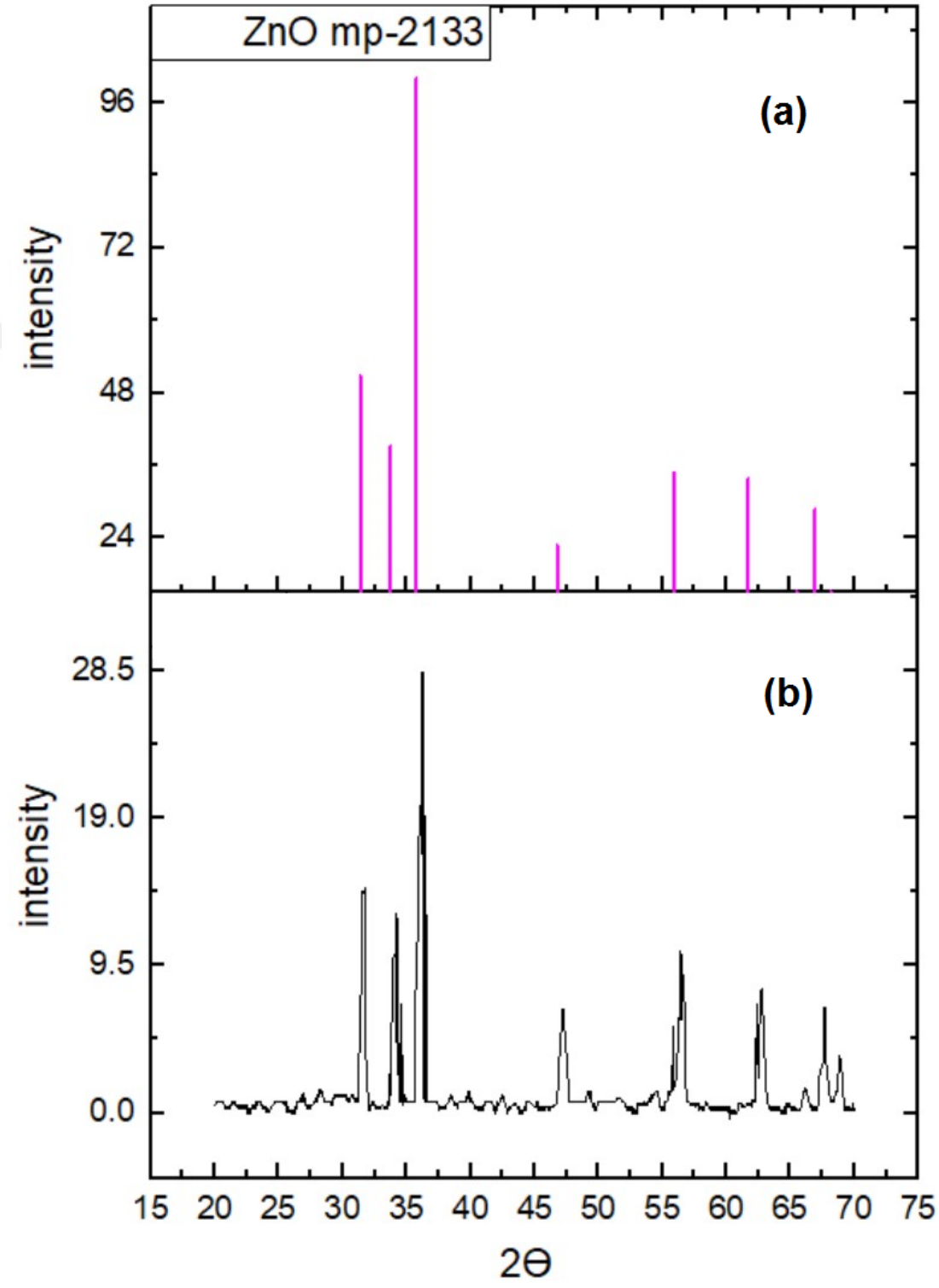

Figure 4.8. The XRD (a) standard, (b) experimental data of undoped ZnO structure.

The XRD pattern is used for identification of crystalline phase and microstructural analysis of the prepared ZnO thin film. The pattern obtained has been indexed as a hexagonal unit cell with wurtzite structure (ICDD Card No. 36-1451) as seen in Figure 4.9. Materials Project online platform was used to match the structure. Figure 4.8 (a) shows the best coherent structure (mp-2133) for the material. It can be observed from Figure 4.8 (b) that zinc oxide films are polycrystalline. The observed relative peak intensities and interplanar spacing have been compared to that of their standard values which is given in Table 4.2. Accordingly, the Miller indices of the crystal planes corresponding to 2□ angle values are given in the Table 4.2.

All peaks of the film correspond to the hexagonal wurtzite structure of ZnO which was studied by many researchers (Rusu et al, 2011; Gu et al, 2004; Prakash et al, 2013; Singh, Vishwakarma, 2015; Singh, Chakrabarti, 2013; Veer et al, 2017). The XRD response of the film corresponding to the (100), (002), and (101) planes become more evidenced. The indexed diffraction peaks were used to calculate the interplanar spacings, **d** corresponding to the planes of the hexagonal (wurtzite) ZnO crystalline structure from Braggs Law, Equation 5. The crystallite sizes of all Miller indices were calculated from the Debye–Scherrer formula, Equation 6. Table 4.2 presents the calculated crystallite size and interplanar spacing values of ZnO film. The average crystallite size is calculated as about 23 nm. The highest relative error of **d** was calculated as 1.449%. In other words, since this error can easily be ignored, it shows that the zinc oxide structure predicted by the ICDD standard and the film prepared in this thesis have the same structure.

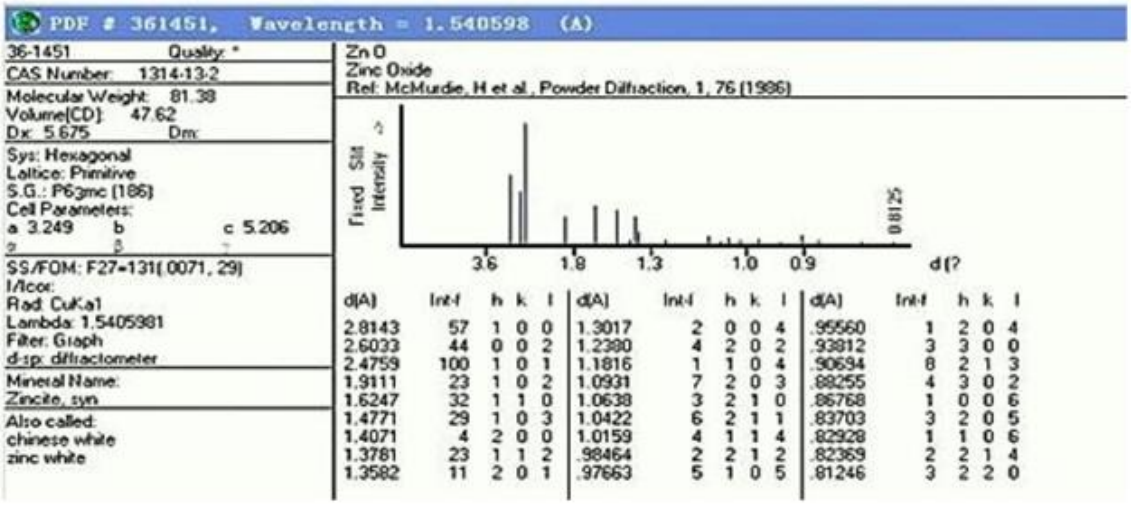

Figure 4.9. The standard of ICDD X-ray Powder Diffraction data belongs to Zinc Oxide structure.

Re-arranging the Williamson-Hall Equation, Equation 9 yields

$$\beta_{hkl} \cos\theta = K\lambda / L + 4\varepsilon \sin\theta \quad \text{.....(10)}$$

which is an equation of a straight line. Equation 10 gives the information about the isotropic nature of the crystals. Figure 4.10 shows the plotting of the Equation 10, with the term ($4\sin\theta$) along the apsis and ($\beta_{hkl} \cos\theta$) along the ordinate axes corresponding to each diffraction peak for ZnO film. This plotted straight line is a good fitted line, corresponding to all the values, as the correlation coefficient value of R^2 is 0.9953. The slope of this straight line provides the value of the intrinsic strain, ε whereas the intercept gives the average particle size of the ZnO film. The origin of the lattice strain is attributed mainly to the lattice expansion or lattice contraction in the nanocrystals due to size confinement, because the atomic arrangement gets slightly modified due to size confinement, compared to their bulk counterpart. On the other hand, many defects also get created at the lattice structure due to the size confinement and this in turn results in the lattice strain (Nath et al, 2019). The negative slope of the fitted line in a Williamson-Hall plot indicates the presence of a compressive strain in the crystal lattice of the specimen, while a positive slope indicates a tensile strain (Singh, Vishwakarma, 2015). The average particle size has been determined from this plot approximately as 19 nm. From the slope, intrinsic strain, ε has been calculated as -0,0013. Since the slope is negative in Figure 4.10, the intrinsic strain is a compressive strain in the crystal lattice.

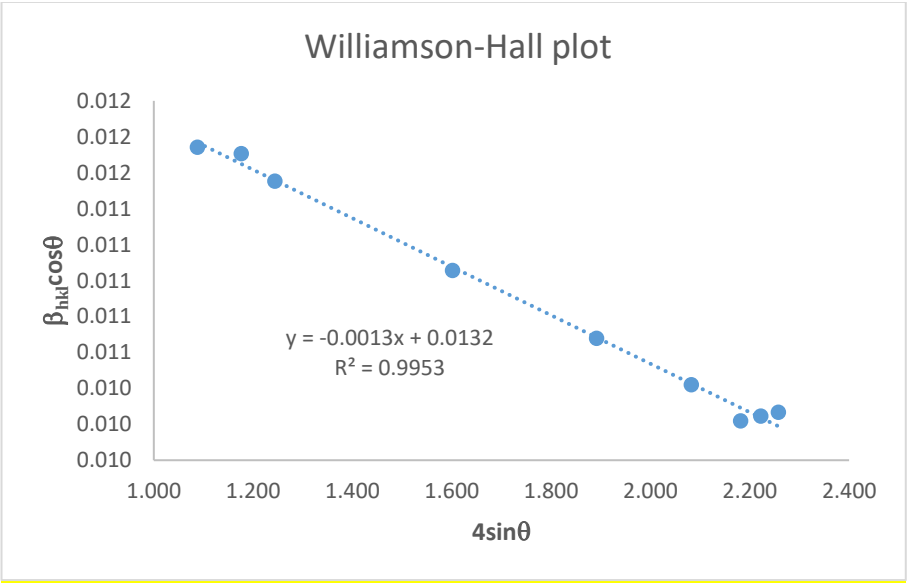

Figure 4.10. Williamson-Hall plot of ZnO film.

Table 4.2. The calculations of the crystallite size, spacing between the planes from the XRD data of ZnO/MoS_2 transparent oxides.

Peak position	FWHM	Crystallite Size	calculated from Bragg's Law	ICDD theoretical value			Relative error of d (%)		
2θ (°)	β hkl (°)	L (nm)	d (Å)	hkl	2θ	d (Å)		4sinθ	βcosθ
31,556	0,699	21,545	2,835	101	31,405	2,848	0,455	1,088	0,012
34,186	0,702	21,609	2,623	002	33,780	2,653	1,139	1,176	0,012
36,222	0,696	21,897	2,480	101	35,777	2,510	1,200	1,243	0,012
47,192	0,691	22,880	1,926	102	46,790	1,942	0,831	1,601	0,011
56,433	0,694	23,688	1,630	110	55,909	1,645	0,884	1,891	0,011
62,724	0,699	24,276	1,481	103	61,729	1,503	1,449	2,082	0,010
66,105	0,698	24,756	1,413	200	65,543	1,424	0,743	2,182	0,010
67,493	0,706	24,692	1,388	112	66,941	1,398	0,737	2,222	0,010
68,707	0,713	24,637	1,366	201	68,173	1,376	0,719	2,257	0,010
	Lavg= 23,331 nm								

The substitutional doping with very low doping concentrations decreases the bandgap. However, if the concentration increases such that it forms a mixed material the band gap may increase. The concept of the resultant band gap by mixing two semiconductors that is the resultant band gap will have an intermediate value. Doping may affect the optical band gap to be high or low. The optical band gap increases or decreases according to the density of localized states; low or high respectively. XRD, SEM and TEM are useful techniques to produce the details of localized states.

4.3. SHEET RESISTANCE MEASUREMENT

To determine the sheet resistance of the ZnO films with various MoS_2 amounts in square geometry, the four-point probe method was used. The sheet resistance of the ZnO films for different MoS_2 amounts is shown in Figure 4.11. The sheet resistance of the composite films decreased from 118.1 to 2.8 Ω/□ as the MoS_2 amount increased from 0 to 4 mg. Additionally, the sheet resistance value is very important parameter for the improvement of electrical conductivity mechanism of the ZnO/MoS_2 composite films due to the generation of more donor levels and the increase in free charge carriers. When MoS_2 was doped with ZnO; Mo, and S atoms merge into the ZnO lattice, and then free charge carriers increase in composite films. This change in structure contributes to the conductivity that decreases the sheet resistance of composite films.

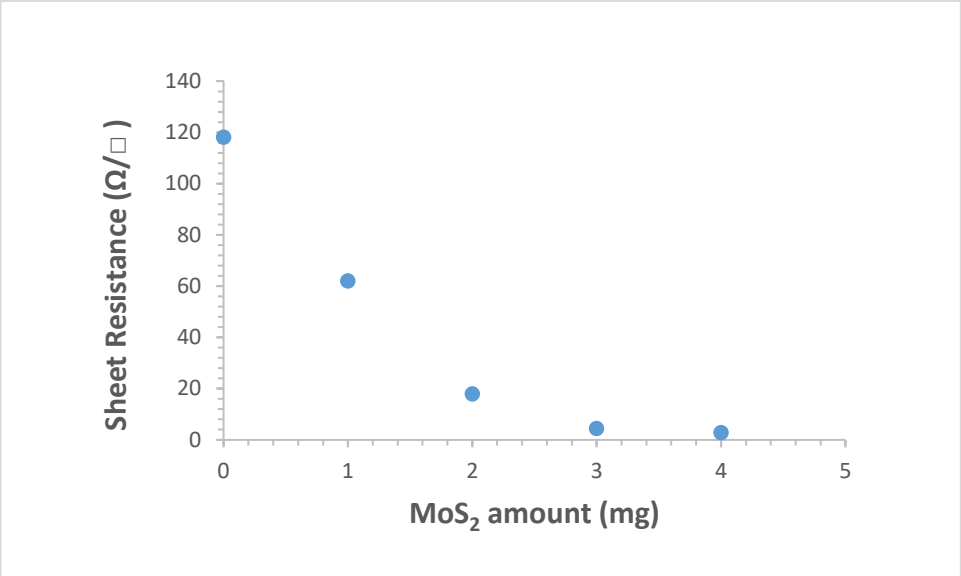

Figure 4.11. Sheet resistance of ZnO/MoS_2 composite films with respect to MoS_2 amount.

The decrease in conductivity also results in a decrease in the optical transmittance of ZnO / MoS_2 composite films as shown in Fig.4.12.

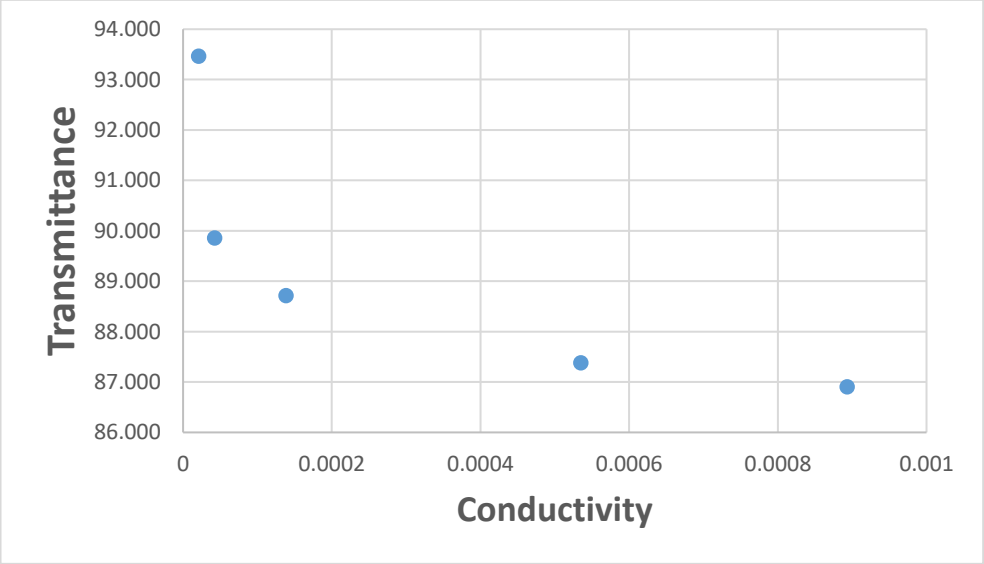

Figure 4.12. Transmittance vs Conductivity of ZnO/MoS_2 composite films.

Although the sheet resistance value is an important parameter, it does not make much sense on its own for transparent conductive films. For this reason, it is necessary to evaluate the transmittance percentage of the film together with the sheet resistance value. With the Haacke's definition (Equation 4), these two parameters can be accurately calculated. The figure of merit value can be evaluated for the presence of an effective transparent conductor. The transparent conductor characteristics of ZnO/MoS_2 composite films is given in Table 4.3. Compared to the FoM values in Table 2.1 which covers the previous studies on various material-doped ZnO transparent conductive oxides, it is possible to conclude that these new films have a structure very similar to the transparent conductivity characteristics of other films, even superior to them for some MoS_2 amounts. The film thickness was varied in the range from 382 nm to 429 nm. It was measured that the ZnO/MoS_2 composite film thickness did not change significantly according to the amount of MoS_2. These composite films can doubtfully be used in all areas where transparent conductors are used.

Table 4.3. Transparent conductor characteristics of ZnO/MoS_2 composite films.

MoS_2 amount (mg)	Film thickness (nm)	Sheet Resistance (Ω/□)	Transmittance (%) at 550 nm	Figure of Merit (FoM)
0	412	118,112	93,464	4,31E-03
1	382	62,014	89,860	5,54E-03
2	405	17,857	88,715	1,69E-02
3	429	4,358	87,381	5,96E-02
4	394	2,842	86,907	8,65E-02

5. CONCLUSION

In this work, ZnO/ MoS_2 composite films with various MoS_2 amounts were fabricated by sol-gel method in order to study the structural, optical and electrical properties of composite film. After all films were heat-treated, absorption measurements were performed with UV-vis spectrophotometer. Due to the characteristics of the spectrophotometer used, the absorbance behavior of the films was measured using corning glass as a reference. Therefore, the absorbance-wavelength data obtained only belong to the prepared film. The optical studies confirm the good dispersion of MoS_2 in ZnO film structure. Under the curve area and normalized width data verify the good performance of composite film were fabricated. The proper ultrasonication process has been realized so as to maintain the good dispersion of the MoS_2 inside the ZnO matrix lowering the normalized width and increasing the resonance ratio. The best dispersion is obtained for the ZnO film with the MoS_2 amount of 4 mg.

Structural investigations showed that the zinc oxide films are polycrystalline and have a wurtzite (hexagonal) structure. The intrinsic strain value was found to be 0.0013 which is comparable result for zinc oxide composites. The negative slope of the fitted line in a Williamson-Hall plot indicates the presence of a compressive strain in the crystal lattice of the specimen, while a positive slope indicates a tensile strain. The average particle size has been determined from this plot approximately as 19 nm. From the slope, intrinsic strain, ε has been calculated as -0,0013. Since the slope is negative, the intrinsic strain is a compressive strain in the crystal lattice. As a new work in the future, it may be interesting to check the mechanical properties by coating these films on a flexible substrate rather than a glass substrate.

The transmittance of the films has a range between 87 to 93 % at the wavelength of 550 nm. The films are transparent in the visible region. This result allows them to be used as transparent oxides. The film thickness was varied in the range from 382 nm to 429 nm. Moreover, the sheet resistance values of the composite films are in the range between 118.1 to 2.8 Ω/□.

The figure of merit used to show the quality of TCO. Haacke's equation was used to calculate FoM and compared the result with current literature studies. TCO films

produced cost-effectively with simpler and easier processes have the same order of magnitude of FoM value (10^{-3}) as the PLD processed films and even better than them for the films with high MoS2 amounts (the order of magnitude for FoM is (10^{-2}) appears to be. This result proves that the films produced are promising composite films to be used as transparent conductors. By using the four-point probe method, the ZnO/MoS_2 film recorded low sheet resistance for charges moving, which is qualificator it to use in photovoltaic applications. The findings demonstrate that one of the successful options for the optoelectronic devices which need large area to applicate may be the MoS_2/ZnO composite. This study provides a new approach to identify the dispersibility from the optical properties, and alter the figure of merit which can be used for further optoelectronic applications.

BIBLIOGRAPHY

Adedokun, O. (2018). 'Review on Transparent Conductive Oxides Thin Films deposited by Sol-gel spin coating technique', *International Journal of Engineering Science and Application*, pp. 88–97.

Adnan, R., Razana, N.A., Ab Rahman, I. and Farrukh, M.A. (2010). 'Synthesis and Characterization of High Surface Area Tin Oxide Nanoparticles via the Sol-Gel Method as a Catalyst for the Hydrogenation of Styrene', *Journal of the Chinese Chemical Society*, Vol. 57, 222-229.

Alam, M. and Cameron, D., (2000). 'Optical and electrical properties of transparent conductive ITO thin films deposited by sol–gel process'. *Thin Solid Films*, 377-378, pp.455-459.

Ali, D., Butt, M. Z., Coughlan, C., Caffrey, D., Shvets, I. V., and Fleischer, K. (2018). 'Nitrogen grain-boundary passivation of In-doped ZnO transparent conducting oxide', *Physical Review Materials*, 2(4), pp. 1–10. doi: 10.1103/PhysRevMaterials.2.043402.

Arca, E., Fleischer, K., Shvets, I.V. (2012). 'An alternative fluorine precursor for the synthesis of SnO_2:F by spray pyrolysis' *Thin Solid Films*, 520.

Bragg, W. H., Bragg, W. L. (1913) 'The Reflexion of X-rays by Crystals'. *Proc. R. Soc. Lond. A.* 88 (605) 428–38.

Dawood, Y.Z., Hassoni, M.H., Mohamad, M.S. (2014) 'Effect of Solution Concentration on Some Optical Properties of Indium Oxide Doped with SnO2 Thin Films Prepared by Chemical Spray Pyrolysis Technique', *International Journal of Pure and Applied Physics* 2, 1.

Garza-Guadarrama, V. De La, Sanchez-Juarez, A., Tiburcio-Silver, A., Ortiz, A. (2001). 'Growth and characterization of SnOx:F thin films prepared by pyrolysis of $SnCl_2$', *Journal of Material Science Letters*, 20.

Gu, F., Wang, S. F., Lü, M. K., Zhou, G. J., Xu, D., & Yuan, D. R. (2004). Structure Evaluation and Highly Enhanced Luminescence of Dy3+-Doped ZnO Nanocrystals by Li+Doping via Combustion Method. Langmuir, 20(9), 3528–3531. doi:10.1021/la049874f

Haacke, G. (1976). 'New figure of merit for transparent conductors', *Journal of Applied Physics*, 47(9), pp. 4086–4089. doi: 10.1063/1.323240.

Hsu, H., Lin, D., Lu, G., Ko, T. and Chen, H., (2018). 'Optical and electrical transport properties of ZnO/MoS2 heterojunction p-n structure'. *Materials Chemistry and Physics*, 220, pp. 433-440.

Hun, S., Na, B., Dong-Geun, D., Jin-Hyo, J. and Donggeun, D., (2007). 'Al-ZnO Thin Films as Transparent Conductive Oxides: Synthesis, Characterization, and Application

Tests'. *Journal of the Korean Physical Society*, 50(3), pp. 622.

Jiamprasertboon, A., Dixon, S., Sathasivam, S., Powell, M., Lu, Y., Siritanon, T. and Carmalt, C., (2019). 'Low-Cost One-Step Fabrication of Highly Conductive ZnO:Cl Transparent Thin Films with Tunable Photocatalytic Properties via Aerosol-Assisted Chemical Vapor Deposition'. *ACS Applied Electronic Materials*, 1(8), pp.1408-1417.

Kim, A., Won, Y. (2013). 'Highly Transparent Low Resistance ZnO/Ag Nanowire/ZnO Composite Electrode for Thin Film Solar Cells', *ACS Nano*, 7, 2, 1081–1091.

Kumara, G.R.A., Ranasinghe, C.S.K., Jayaweera, E.N., Bandara, H.M.N., Okuya, M. and Rajapakse, R.M.G. (2014). 'Preparation of Fluoride-doped Tin Oxide Films on Soda-lime Glass Substrates by Atomized Spray Pyrolysis Technique and their Subsequent Use in Dye-sensitized Solar Cells', *Journal of Physical Chemistry*, C118: 16 479-16 485.

Lei, M., Liu, C., Zhou, Y., Yan, Z., Han, S., Liu, W., Xiang, X. and Zu, X. (2016). 'Microstructure and photoluminescence of MoS_2 decorated ZnO nanorods'. *Chinese Journal of Physics*, 54(1), pp.51-59.

Liu, Y., Li, Y. and Zeng, H. (2013). 'ZnO-Based Transparent Conductive Thin Films: Doping, Performance', and Processing. *Journal of Nanomaterials*, pp.1-9.

Lu, J. G., Fujita, S., Kawaharamura T., Nishinaka, H., Kamada, Y., Ohshima, T., Ye, Z. Z., Zeng, Y. J., Zhang, Y. Z., Zhu, L. P., He, H. P., and Zhao, B. H. (2007) "Carrier concentration dependence of band gap shift in n -type ZnO:Al films," *Journal of Applied Physics*, 101, no. 8, 083705,1-7.

Mahroug, A., Boudjadar, S., Hamrit, S. and Guerbous, L., (2014). 'Structural, optical and photocurrent properties of undoped and Al-doped ZnO thin films deposited by sol–gel spin coating technique'. *Materials Letters*, 134, pp. 248-251.

Manoj, P.K., Joseph, B., Vaidyan, V.K. and Amma, D.S.D. (2007). 'Preparation and characterization of indium-doped tin oxide thin films', *Ceramics International*, Vol. 33, 273-278.

Mokhtar, H., Faouzi, G., Lassaad, E. (2014). 'Characterization of ITO Thin Films Prepared by Sol-gel Spin-Coating Technique', *Sensors & Transducers*, Vol. 27, Special Issue.

Nath, D., Singh, F., and Das, R. (2019). 'X-Ray Diffraction Analysis by Williamson-Hall, Halder-Wagner and Size-Strain Plot Methods of CdSe Nanoparticles- A comparative study'. *Materials Chemistry and Physics*, 122021.

Njuguna, J., Vanli, O. A. and Liang, R. (2015). 'A Review of Spectral Methods for Dispersion Characterization of Carbon Nanotubes in Aqueous Suspensions', *Journal of Spectroscopy*. doi: 10.1155/2015/463156.

Prakash, T., Jayaprakash, R., Neri, G., Kumar, S. "Synthesis of ZnO Nanostructures by Microwave Irradiation Using Albumen as a Template", Journal of

Nanoparticles, vol. 2013, ArticleID 274894, 8 pages, 2013. https://doi.org/10.1155/2013/274894

Putritama, V., Fauzia, V. and Supangat, A., (2020). 'The effect of the layer number of MoS2 nanosheets on the photocatalytic efficiency of ZnO/MoS_2'. *Surfaces and Interfaces*, 21, p.100745.

Rathnasamy, R., Santhanam, M. and Alagan, V., (2018). 'Anchoring of ZnO nanoparticles on exfoliated MoS_2 nanosheets for enhanced photocatalytic decolorization of methyl red dye'. *Materials Science in Semiconductor Processing*, 85, pp.59-67.

Rusu, D.I., Rusu, G.G., and Luca, D. Structural Characteristics and Optical Properties of Thermally Oxidized Zinc Films (2011) ACTA PHYSICA POLONICA A Vol. 119 No. 6, 850-856.

Scherrer, P. (1918) 'Bestimmung der Grösse und der inneren Struktur von Kolloidteilchen mittels Röntgenstrahlen', *Nachr. Ges. Wiss. Göttingen* 26, pp. 98-100.

Singh, A., Vishwakarma, H. L. (2015). Study of structural, morphological, optical and electroluminescent properties of undoped ZnO nanorods grown by a simple chemical precipitation. Materials Science-Poland, 33(4), 751–759. doi:10.1515/msp-2015-0112

Singh, S., & Chakrabarti, P. (2013). Comparison of the structural and optical properties of ZnO thin films deposited by three different methods for optoelectronic applications. Superlattices and Microstructures, 64, 283–293. doi:10.1016/j.spmi.2013.09.031

Smith, A., Laurent, J.M., Smith, D.S., Bonnet, J.P. and Clemente, R.R. (1995). 'Relation between solution chemistry and morphology of SnO_2-based thin films deposited by a pyrosol process', *Thin Solid Films*, 266.

Stoica, T.F., Stoica, T.A., Zaharescua, M., Popescu, M., Sava, F., Popescu-Pogrion, N., Frunza, L. (2000). 'Characterization of ITO Thin Films Prepared by Spinning Deposition Starting from a Sol-Gel Process', *Journal of Optoelectronics and Advanced Materials* Vol. 2, No. 5.

Tan, Y., and Resasco, D.E. (2005) Dispersion of Single-Walled Carbon Nanotubes of Narrow Diameter Distribution, *J. Phys. Chem. B* 2005, *109*, 14454-14460.

Tonny, K.N., Rafique, R., Sharmin, A., Bashar, M.S., and Mahmood, Z.H. (2018). 'Electrical, optical and structural properties of transparent conducting Al doped ZnO (AZO) deposited by sol-gel spin coating', *AIP Advances*, 8(6). doi: 10.1063/1.5023020.

Veer, D., Singh, R. M., & Kumar, H. (2017). 'Structural and Optical Characterization of ZnO-TiO2-SiO2 Nanocomposites Synthesized by Sol-Gel Technique'. *Asian Journal of Chemistry*, 29(11), 2391–2395. doi:10.14233/ajchem.2017.20690

Wang, J., Deng, J., Li, Y., Yuan, H. and Xu, M., (2020). 'ZnO nanocrystal-coated MoS2 nanosheets with enhanced ultraviolet light gas sensitive activity studied by surface photovoltage technique'. *Ceramics International*, 46(8), pp.11427-11431.

Williamson, G., Hall, W. (1953). 'X-ray line broadening from filed aluminium and wolfram'. *Acta Metallurgica*, 1(1), 22–31. doi:10.1016/0001-6160(53)90006-6

Wu, H., Jile, H., Chen, Z., Xu, D., Yi, Z., Chen, X., Chen, J., Yao, W., Wu, P. and Yi, Y., (2020). 'Fabrication of ZnO@MoS2 Nanocomposite Heterojunction Arrays and Their Photoelectric Properties'. Micromachines, 11(2), p.189.

Zhao, D., Sathasivam, S., Li, J. and Carmalt, C., (2019). 'Transparent and Conductive Molybdenum-Doped ZnO Thin Films via Chemical Vapor Deposition'. *ACS Applied Electronic Materials*, 2(1), pp.120-125.

International Centre for Diffraction Data (ICDD) Official Web Site: https://www.icdd.com/?gclid=Cj0KCQiA6t6ABhDMARIsAONIYyyW3wt2WBi-PQdQmnh5tYvXaV3cA265VNLLYEyj5x2DtBWPO9K33EwaAs91EALw_wcB

Materials Project Online Platform: https://materialsproject.org/materials/mp-2133/

CURRICULUM VITAE

Name and Surname: Shahad Tareq

Academic Background
Bachelor's Degree Education: Laser Engineering
Post Graduate Education: High Diploma in laser and Optoelectronics Engineering
Foreign Languages: English

Work Experience
Institutions Served and Their Dates: Teacher of Optoelectronics laboratory between 2010-2017.